INTERACTIONS OF METAL-BASED ENGINEERED NANOPARTICLES WITH AQUATIC HIGHER PLANTS: A REVIEW OF THE STATE OF CURRENT KNOWLEDGE

MELUSI THWALA,†‡ STEPHEN J. KLAINE,§|| and NDEKE MUSEE*#

† Source Directed Scientific Measures Research Group, Council for Scientific and Industrial Research, Pretoria, South Africa

‡ Zoology Department, University of Johannesburg, Johannesburg, South Africa

§ Department of Biological Sciences, Clemson University, Clemson, South Carolina, USA

|| School of Biological Sciences, North-West University, Potchefstroom, South Africa

Department of Chemical Engineering, University of Pretoria, Pretoria, South Africa

Abstract: The rising potential for the release of engineered nanoparticles (ENPs) into aquatic environments requires evaluation of risks in order to protect ecological health. The present review examines knowledge pertaining to the interactions of metal-based ENPs with aquatic higher plants, identifies information gaps, and raises considerations for future research to advance knowledge on the subject. The discussion focuses on ENPs' bioaccessibility; uptake, adsorption, translocation, and bioaccumulation; and toxicity effects on aquatic higher plants. An information deficit surrounds the uptake of ENPs and associated dynamics, because the influence of ENP characteristics and water quality conditions has not been well documented. Dissolution appears to be a key mechanism driving bioaccumulation of ENPs, whereas nanoparticulates often adsorb to plant surfaces with minimal internalization. However, few reports document the

internalization of ENPs by plants; thus, the role of nanoparticulates' internalization in bioaccumulation and toxicity remains unclear, requiring further investigation. The toxicities of metal-based ENPs mainly have been associated with dissolution as a predominant mechanism, although nano toxicity has also been reported. To advance knowledge in this domain, future investigations need to integrate the influence of ENP characteristics and water physicochemical parameters, as their interplay determines ENP bioaccessibility and influences their risk to health of aquatic higher plants. Furthermore, harmonization of test protocols is recommended for fast tracking the generation of comparable data.

Keywords: Engineered nanoparticles, Aquatic plants, Bioaccessibility, Bioaccumulation, Nanoecotoxicology

* Address correspondence to ndeke.musee@up.ac.za.

Published online XXX in Wiley Online Library (www.wileyonlinelibrary.com).

DOI: 10.1002/etc.3364

INTRODUCTION

Concerns about the environmental health and safety of engineered nanomaterials (ENMs) emerged in the early 2000s as a result of uncertainties surrounding interactions with organisms and reports of enhanced toxicity potential at nano scale [1–4]. For example, as a result of nano-scale dimensions, ENMs exhibit special physicochemical properties, such as large surface area to mass ratio, high surface energy, and high reactivity [5,6], that distinguish them from bulk-scale counterparts. Classes of ENMs are diverse and include carbon-based, quantum dots, metal, and

metal oxide nanoparticles. The focus of the present review is specific to metal-based engineered nanoparticles (ENPs). Herein the term "metal-based ENPs" collectively refers to both metals and metal oxide counterparts. This category of ENPs is the exclusive focus of the present review because of their distinctive characteristics, such as magnetism, catalytic capacity, and optoelectronic properties. Another important property is dissolution potential, or the potential to release soluble metal species as free ions or metal complexes. The useful properties of metal-based ENPs mean that they are widely produced and incorporated into consumer products and industrial applications [7,8], and they are consequently increasingly being released into human-made [9–11] and natural [12] aquatic systems.

The unique nano-scale properties of ENPs mean that their environmental fate, behavior, and toxicity may differ from those of bulk-scale pollutants [13] such that traditional hazard and risk assessment models are no longer adequate. Research efforts to date have concentrated on gaining insight into the environmental implications of nanotechnology—for example, with respect to fate, transport, and toxicological effects of ENPs—which currently lag behind production and application efforts [14]. Thus, the rapid increase in production of ENPs and ultimate incorporation into nano-enabled products have triggered a need for information on the potential environmental effects of nano scale pollutants. Such information is essential for the development of a sound risk-assessment framework and, in turn, can inform the adoption of safe-by-design approaches for future nano-enabled products.

Insufficient data and knowledge on the biological effects of ENMs has fostered the birth of nanotoxicology [3,15], which initially focused on establishing the effects of ENMs on humans [3,4,16–18]. Later, concerns emerged about the potential environmental effects of ENMs [2,19–21], leading to the development of nanoecotoxicology [22] as a branch of nanotoxicology that

chiefly focuses on the ecological health aspects of ENMs [22–24]. Fewer than 50 open peer-reviewed nanoecotoxicity studies had been reported by 2008 [17], when Klaine et al. [25] published a comprehensive review of nanoecotoxicology research. Since then, the number of published nanoecotoxicology studies has increased rapidly [14,22], and numerous excellent reviews focusing on the fate, behavior, and toxic effects of ENPs have been published. Reviews cover the toxicity of ENPs to bacteria [26–29], algae [26,29–31], invertebrates [26,32–35], and fish [24,36–38], as well as the fate and behavior of ENPs in aquatic systems (see the *Bioaccessibility* section). To the knowledge of the authors, no nanoecotoxicology review is available for aquatic higher plants, hence the focus of the present article on the interactions of metal-based ENPs with aquatic higher plants.

Aquatic higher plants, also known as aquatic vascular plants, include free-floating or rooted and emergent or submerged plants. Aquatic higher plants occupy a key position in ecological energy metabolism as producers and food sources, and they shelter a variety of invertebrates [39]. Little nanoecotoxicity information is available for aquatic higher plants as opposed to microalgal species and terrestrial higher plants, including agricultural crops [25,40–44]. The possibility exists that aquatic plants have the potential to bioaccumulate ENPs and transfer them between trophic levels in aquatic ecosystems [45]. Assessment of the risk posed by ENPs in aquatic environments therefore requires data at different trophic levels [46]. Overall, the present review on the interaction of ENPs with aquatic higher plants deals with aspects of bioavailability; uptake, translocation, and accumulation; and toxicity effects. The review generates an information portfolio on current knowledge about the interactions of metal-based ENPs with aquatic higher plants. Furthermore, it makes recommendations for future research directions that will help strategize and prioritize knowledge generation, through screening of

patterns or commonalities in the current reported information.

BIOACCESSIBILITY

The interactions of ENPs with aquatic higher plants are complex and dynamic. Several key physicochemical processes influence the amount and form of ENPs that interact with aquatic organisms including plants, as summarized here. Note that the concept of "bioaccessible proportion" used in the present article refers to the proportion of ENPs available for interacting with the plant surface and potentially available for uptake [47].

The behavior, fate, and transport of ENPs in aquatic systems are influenced by their physical and chemical traits, such as size, shape, surface charge potential, crystal structure, composition, and surface coating. In aquatic systems, ENPs undergo numerous transformations as a result of biotic and abiotic factors, which consequently determine ENP bioaccessibility, uptake, bioavailability, and toxicity potential upon interaction with aquatic biota [48,49]. Therefore, aquatic biota encounter or interact with transformed, rather than pristine, ENPs after their release into aquatic environments [50,51]. Metal-based ENPs undergo a number of transformations in aqueous media (Figure 1). The present review highlights the relevance of interactions of ENPs with aquatic plants, as the environmental behavior of ENPs has been addressed in detail elsewhere [29,49,50,52,53].

For metal-based ENPs, a key determinant of their environmental fate is dissolution potential. The release of dissolved metallic forms or ions from metal-based ENPs is a chemical trait often enhanced with diminishing nano-scale size, which in turn increases their reactivity [52]. Thus, the following forms of metal-based ENPs interact with biota: dissolved metals, new chemical substances formed after interacting with biotic and abiotic aquatic factors, and

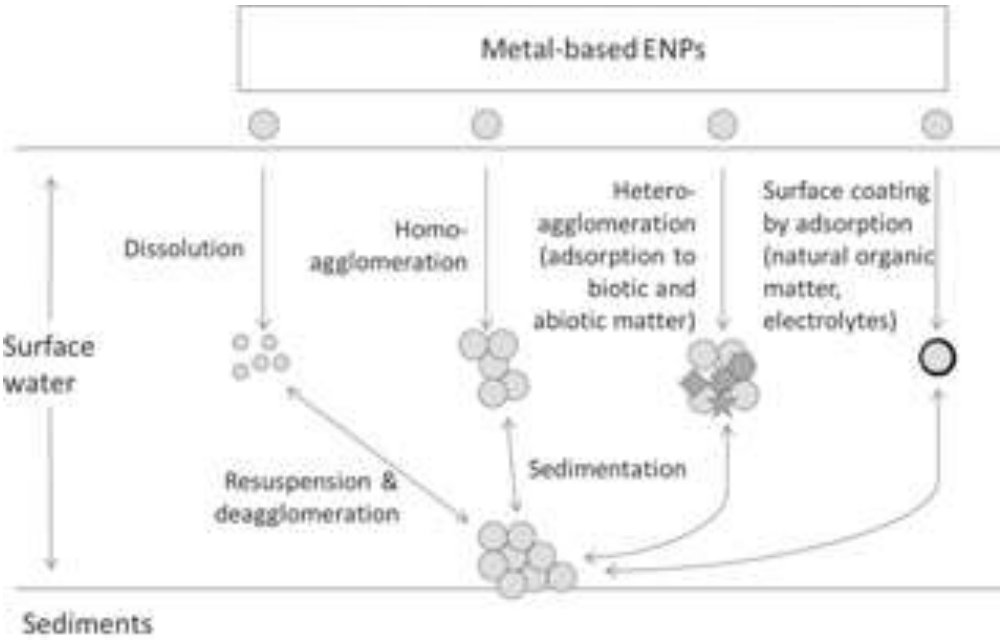

Figure 1. Schematic presentation of transformations that metal-based engineered nanoparticles (ENPs) undergo in aqueous environments. These are among key processes that determine the behavior (chemical and physical) and bioavailability of metal-based ENPs in aquatic ecosystems

particulates [43]. Therefore, each study needs to pay attention to the bioaccessible fractions of metal-based ENPs as a result of associated implications for uptake and toxicity. Already there are suggestions that uptake [42,45,54–56] and toxicity [44,53,57,58] of metal-based ENPs are dependent on their physicochemical characteristics.

In aqueous suspension, metal-based ENPs often agglomerate, where gravitational forces may overcome buoyancy, causing sedimentation of particles and thereby reducing exposure concentration [29,44]. However, often overlooked is the opposite effect of deagglomeration, as the transformation of ENPs is dynamic and multidimensional. Chemical processes such as reduction of metal cations (e.g., Ag^{+}) can result in the formation of smaller secondary particles in suspension [59], thereby introducing new bioaccessible size states. Changes in the size of ENPs are important for determining exposure size (bioaccessible size) and persistence in aqueous

systems.

The interplay of agglomeration, deagglomeration, sedimentation, and resuspension of ENPs (Figure 1) has implications for free-floating and rooted aquatic plants, causing spatial and temporal variation of exposure scenarios. Settling of ENPs onto sediments may purify aquatic systems of such contaminants [60], but this argument overlooks the fact that aquatic systems are not 1-dimensional. For instance, ENPs can dissolve or deagglomerate during resuspension and still interact with pelagic biota. These and other case studies are discussed below (see the *Adsorption, Uptake, and Bioaccumulation* and *Toxicity Effects* sections), regarding their influence on uptake and toxicity. The physicochemical properties of aquatic environments—such as pH, ionic strength, inorganic constituents, total organic matter—are important in the transformation of ENPs. These properties may alter bioaccessible size and surface properties or influence dissolution rate. Transformations such as these exert influence on the bioaccessible state of ENPs to aquatic biota in general. Detailed accounts of the aquatic fate and behavior of ENPs have been reported elsewhere [25,40,49,52,53,61–64] and are outside the scope of the present article. Generally, the dissolution rate of metal-based ENPs is pH-dependent [64,65], suggesting that varying pH regimes will present different bioaccessibility of ENPs to aquatic plants as well.

The toxicity of metals in aquatic environments is largely related to free metal activity or soluble metallic species [66]. Analysis of trace metal speciation involves the determination of metal chemical forms, including free metal ions, inorganic and organic complexes, and organometallic compounds. For example, electrolytes and organic matter control the stability of ENPs as they interact with ENP surfaces, thereby altering surface characteristics such as surface charge potential and coating. When ENPs interact with aquatic higher plants, dissolved organic

carbon (DOC) can increase their bioaccessible size [42], as in the case of gold nanoparticles (AuNPs), where the resultant AuNP–DOC complexes were larger than AuNP and its homoagglomerates, hence limiting uptake potential. Whether in particulate or dissolved form, ENPs interact with higher plants through processes such as adsorption, deposition, and internalization. The fate and toxicity implications have been discussed [49,67–71].

The above information suggests that the bioaccessibility and bioavailability of metal-based ENPs to aquatic higher plants are underpinned by a complex interplay of ENPs and exposure water characteristics. Therefore, integrating ENP characteristics and aqueous properties is necessary when investigating the environmental behavior of ENPs, rather than treating each component separately. Ultimately, the bioavailability of ENPs in aquatic systems is determined by the complex interplay of processes highlighted earlier in this section, which are temporally and spatially dynamic. Factors influencing the bioaccessibility of ENPs are fundamental because, in turn, they determine bioavailability, bioaccumulation, and toxicity toward aquatic higher plants.

ADSORPTION, UPTAKE, AND BIOACCUMULATION

Aquatic plants obtain essential nutrients from the surrounding aquatic matrices, so uptake of ENPs could arise from similar mechanisms [45]. Variability in ENP uptake mechanisms is likely because of physiological, anatomical, and morphological diversity among aquatic higher plants. For example, different uptake mechanisms can result from morphological differences in root [45] and vascular [72] systems between plant species. In the present review, the term "uptake" broadly refers to processes by which ENPs and their derivatives reach the inside of plant tissues or cells through active and passive mechanisms. The term excludes adsorption onto

Table 1. Summary of metal-based ENP accumulation pathways by aquatic higher plants

Uptake pathway	ENP type	Uptake detection method	ENP characteristics	Exposure water	Plant	Ref.
Internalization (tissue)	AuNP	TEM; STEM and SEM; and EDX	4 nm; spherical; ζ –14.1 mV; 250 g/L	Well/borehole water; pH 7.1; TOC 8.56 mg/L; $CaCO_3$ 107 mg/L; conductivity 210 µS/cm	*Myriophyllum simulans*	[45]
Internalization (cellular)	AuNP	TEM; STEM and SEM; and EDX	4 nm; 18 nm; spherical; ζ –14.1 mV; ζ –9.73 mV	Well/borehole water; pH 7.1; TOC 8.56 mg/L; $CaCO_3$ 107 mg/L; conductivity 210 µS/cm	*Azolla caroliniana*	[45]
Adsorption (no internalization)	AuNP	TEM; STEM and SEM; and EDX	4 nm; 18 nm; spherical; ζ –14.1 mV; ζ –9.73 mV	Well/borehole water; pH 7.1; TOC 8.56 mg/L; $CaCO_3$ 107 mg/L; conductivity 210 µS/cm	*Egeria densa*	[45]
Adsorption (no internalization)	TiO_2NP	SEM; TEM	275–2398 nm; SSA 50 m^2/g; 0.01–10 mg/L	Steinburg growth medium; pH 5.5; $CaCO_3$ 166 mg/L	*Lemna minor*	[74]
Adsorption (roots)	CdS QDs	TEM	4.3 nm; ζ –9.8 mV	Hoagland's medium	*Schoenoplectus tabernaemontani*	[75]
Adsorption (roots)	CuONP	TEM	38 nm; SSA 12.84 m^2/g; ζ –2.8 mV	Hoagland's medium	*S. tabernaemontani*	[75]
Tissue and cellular	CdS QDs	TEM	4.3 nm; ζ –9.8 mV	Hoagland's medium	*S. tabernaemontani*	[75]

internalization						
Tissue and cellular internalization	CuONP	TEM	38 ± 7 nm; SSA 12.84 m^2/g; ζ –2.8 mV	Hoagland's medium	*S. tabernaemontani*	[75]
Adsorption	ZnONP	ICP-OES	25 nm; uncoated; SSA 90 m^2/g; 1–10 mg/L	OECD growth medium; pH 6.5	*Salvinia natans*	[58]

ENP = engineered nanoparticle; AuNP = gold nanoparticle; TiO_2NP = titanium oxide nanoparticle; CdS QDs = cadmium sulfide quantum dots; CuONP = copper oxide nanoparticle; ZnOP = zinc oxide nanoparticle; TEM = transmission electron microscopy; STEM = scanning transmission electron microscopy; SEM = scanning electron microscopy; EDX = energy dispersive X-ray spectroscopy; TOC = total organic carbon; SSA = specific surface area; ICP-OES = inductively coupled plasma optical emission spectrometry; OECD = Organisation for Economic Co-operation and Development; ζ = zeta potential

plant surfaces. Therefore, bioaccumulation in this context can occur from internalized (uptake) or adsorbed ENPs and resultant dissolved metallic forms. The mechanisms reported in the context of ENPs' association with aquatic higher plants are summarized in Table 1, excluding the bioaccumulation of dissolved metal forms. Bioaccumulation constitutes an important process during interactions of ENPs with plants because it can be a precursor to toxicological effects if the pollutant's concentration exceeds a certain threshold. Knowledge of the uptake kinetics of ENPs by aquatic plants is incomplete, despite earlier research [41,43,72,73], although it is a key aspect that determines the bioavailability, bioaccumulation, and toxicity of ENPs.

Adsorption

Adsorption is a plausible mechanism for the accumulation of ENPs by aquatic higher plants [45,58,74,75]. For example, electron microscopy techniques (transmission electron microscopy, scanning transmission electron microscopy, and scanning electron microscopy) together with energy-dispersive X-ray spectroscopy, showed the presence of AuNPs adsorbed on root tissue surfaces [45]. For *Egeria densa*, no internalization of AuNPs was observed, which suggested that adsorption was likely the dominant accumulation mechanism; for *Azolla caroliniana* and *Myriophyllum simulans*, however, internalization of AuNPs also occurred. The uptake of AuNPs was higher in *A. caroliniana* than in *M. simulans*. This was attributed to the presence of stomata on both sides of fronds, as well as root hairs, which increase the surface area for uptake, whereas the other 2 species possess limited root hairs. The suggestion that uptake mechanisms differ between species [72] was supported by the findings of Glenn et al. [45].

Using electron microscopy techniques, Li et al. [74] found agglomerates of titanium dioxide nanoparticles (TiO_2NPs) adsorbed onto *Lemna minor* fronds, but no internalization was

evident; they concluded that adsorption was the dominant accumulation mechanism in that investigation. The lack of TiO_2NP internalization by *L. minor* was attributed to the sieving nature of the cell wall pores and the sorption of ENPs to cell surface exudates, which in turn promoted agglomeration. Various epidermal structures and exudate forms (e.g., amino acids, enzymes, or sugars) lining plant cell walls present a layer capable of further transforming ENPs (on interaction) and thus facilitate the uptake of ENPs or even their rejection [76,77]. In addition, ENP internalization through cell wall pores can be regulated by bioaccessible size [78]. Cell wall pores in plants are known to vary in size from about 10 nm to 50 nm [79–81]. Such size ranges raise the possibility that cell wall pores are capable of controlling entry, dependent on the exposure size and other characteristics [78]. In certain cases, however, ENPs can penetrate cells even when they are larger than cell wall pore size, and these mechanisms are discussed below (see *Internalization* section).

Adsorption to the root epidermis as well as tissue and cellular internalization were both found to result in the accumulation of copper oxide nanoparticles (CuONPs) and cadmium sulfide quantum dots (CdS QDs) by *Schoenoplectus tabernaemontani* [75]. However, the predominant driver of the 2 processes was not determined. Furthermore, the contribution of dissolved metal forms to bioaccumulation was not investigated, and therefore, the authors may have incorrectly associated bioaccumulation only with uptake of nano forms. Results indicated that accumulation of CuONPs was rapid compared with CdS QDs, and hence uptake potential was ENP type–dependent, as suggested previously [73,82]. However, Zhang et al. [75] did not account for the reported relatively higher CuONP accumulation compared to CdS QDs. We postulate that accumulation variability probably resulted from preferential assimilation of Cu released from CuONPs since Cu is an essential element in numerous physiological processes

[83,84]. Dissolution analysis could provide more insight into this hypothesis. Internalization of the ENPs was possibly facilitated by endocytosis [85,86] or carrier proteins [73,82,87]. Endocytosis is the active cellular internalization of substances through engulfing by the membrane forming a vacuole. Following exposure of *Salvinia natans* to zinc oxide nanoparticles (ZnONPs), adsorption of ZnONPs/Zn to roots was observed; but internalization was not investigated [58]. Inductively coupled plasma-optical emission spectrometry was used to quantify Zn accumulated in unrinsed and rinsed roots, where it was observed that rinsing resulted in Zn loss. Such findings provided confirmation of ZnONPs/Zn adsorbed to root surfaces.

Adsorption of ENPs to plant surfaces appears to be a key mechanism for their phytoextraction from surrounding water. For instance, some reports [45,58,74] have attributed accumulation of ENPs solely to adsorption, while in other cases adsorption coupled with internalization of nano and dissolved metal forms has been observed [45,75]. Adsorption can drive the accumulation of particulates and dissolved metallic forms from solution; although such a scenario has not been reported, it remains highly probable. This is not unexpected considering that accumulation of metallic species in any physicochemical form will arise initially from physical contact with the plant surface, thus rendering adsorption highly likely. The findings of Glenn et al. [45] and Zhang et al. [75] support this suggestion, as ENPs were shown to be both inside (internalized) and outside (adsorbed) plant tissues.

Internalization

Glenn et al. [45] reported AuNP internalization into the roots of *A. caroliniana*, and *M. simulans*, while no uptake occurred in *E. densa.* Internalization was found to vary with particle size and plant species. In *A. caroliniana*, for example, 4-nm AuNPs were detected at a higher

frequency than 18-nm AuNPs, whereas no internalization of 18-nm AuNPs was detected in *M. simulans*, thus illustrating size-dependent internalization, possibly attributable to cell wall pore size discrimination. Furthermore, relatively higher bioaccumulation of Au was observed in *A. caroliniana*, whereas no uptake was detected in *E. densa*. Using transmission electron microscopy, Glenn et al. [45] demonstrated that changes in root tissue density explained the differences in uptake among the 3 plants. They suggested that the enhanced uptake of AuNPs by *A. caroliniana* was the result of the presence of stomata on both sides of fronds as well as root hairs, which in turn increased the surface area for AuNPs uptake, unlike other species without root hairs. Secondly, higher uptake by *A caroliniana* was also associated with its salt intolerance compared with the salt-tolerant *M. simulans* and *E. densa*, where the latter species have the ability to efficiently control and limit uptake of substances from the surrounding water, including AuNPs in this instance. Higher AuNP internalization by the salt-intolerant *A. caroliniana* can be linked to carrier protein–mediated internalization [73,82], as carrier proteins in plants are active in osmoregulation. The differences in ENP uptake between species observed by Glenn et al. [45] illustrate the role of distinctive morphological and physiological characteristics between species, supporting earlier suggestions by Ma et al. [72].

Zhang et al. [75] investigated the internalization of CuONPs and CdS QDs in the roots of *S. tabernaemontani*. Presence of ENPs in epidermal tissue and within the plant cells was confirmed using electron microscopy techniques coupled with energy-dispersive X-ray spectroscopy. The internalization of ENPs was partly ascribed to endocytosis, considering that CuONPs had a large size of 38 nm but was still detected inside the plant cells. Few reports have documented ENP internalization by aquatic higher plants (Table 1); nonetheless, mechanisms underpinning internalization of ENPs in plants remain poorly understood [41,81,88,89], a data

gap that needs to be addressed in future investigations. Notably, there are suggestions that internalization is mainly facilitated by processes similar to those for nutrients and moisture absorption from the surrounding environment [90,91]. Others [78,90,92,93] have indicated that internalization is facilitated by cell wall pores as they are semipermeable and, therefore, ENPs can pass into the cytoplasm. The cell wall pores are approximately 10 nm to 50 nm in diameter [79–81] and, as such, can permit entry of substances from the environment, including ENPs, into the plant cells depending on bioaccessible size. However, small ENP size alone does not translate into cell wall pore internalization [45,74,81], which points to other mechanisms facilitating internalization.

For example, endocytosis has been suggested to aid the transfer of ENPs into plant cells [85,86], similar to facilitation of other substances into cells. This implies that endocytosis can also facilitate internalization of ENPs larger than cell wall pores, depending on particle properties and orientation [41,93]. However, the selectivity criteria are yet to be established [89]. Finally, binding of ENPs onto carrier proteins and organic chemicals also has been proposed [73,82,87]. For instance, metallothioneins can facilitate assimilation of metal-based ENPs [89]. The size of ENPs is a key determinant for their internalization by aquatic higher plants [45]—smaller forms tend to be internalized rapidly. Size is the only characteristic that has so far been reported to influence the internalization of ENPs in nano form by aquatic higher plants. However, caution is raised against the general assumption of higher internalization rate for smaller ENPs solely based on their size. Rather, a complex set of plant characteristics, water physicochemical parameters, and ENP properties interactively determine internalization potential. Internalization kinetics is therefore a topic warranting further research.

Bioaccumulation and translocation

Bioaccumulation analysis is among the methods used in determining the bioavailability of metal-based ENPs to aquatic biota by quantifying biomass metal content. An example is the quantification of total Zn in plants after exposure to ZnONPs. Besides being an indicator of ENP bioavailability, bioaccumulation is a measure of the potential for bioconcentration and trophic transfer [45,94]. Bioaccumulation is also a potential method for phytoextraction of nano pollutants in wastewater treatment systems [75], an application commonly used for bioremediation of metal-contaminated waters [95,96]. Bioaccumulation remains a valuable indicator of metal contamination. Reports of metal bioaccumulation by aquatic higher plants exposed to metal-based ENPs are listed in Table 2. Importantly, bioaccumulation analysis will not normally reveal the underlying driving processes (uptake vs adsorption), but assumptions can be derived from characterization of ENPs, water chemistry, and knowledge of plant species physiology. Furthermore, discrimination between accumulation of dissolved metal forms and ENPs is often challenging, though dissolution analysis of the exposure water can provide insights into this aspect.

ZnONPs. In the study by Hu et al. [55], the duckweed *Spirodela polyrhiza* was exposed to ZnONPs (1 mg/L, 10 mg/L, and 50 mg/L) and $ZnSO_4$ (3.5 mg/L) for 96 h. Zinc bioaccumulation in plants exposed to ZnONPs was directly related to exposure concentration. Whole-plant Zn concentrations were approximately 2 mg/g to 4.5 mg/g from ZnONP exposures and 4.5 mg/g from soluble Zn exposure ($ZnSO_4$). Therefore, Zn bioaccumulation was rapid in soluble Zn exposures compared to nano counterparts. Dissolution analysis of ZnONPs indicated that Zn was predominantly bioaccessible in the dissolved form, as the ENPs rapidly agglomerated up to approximately 4 μm (average 130 nm). The larger particles were deemed too

Table 2. Summary findings on the bioaccumulation of ENPs by aquatic higher plants

ENP	ENP characteristics	Exposure concentration	Exposure water	Exposure duration	Bioaccumulation	Plant	Ref.
ZnONP	25 nm; SSA 90 m^2/g	1–50 mg/L	Hoagland's medium; pH 6.5	96 h	2–4.5 mg/g (whole plants) (est.)	*Spirdoela polyrhiza*	[55]
ZnONP	25 nm; SSA 90 m^2/g	1–50 mg/L	Hoagland's medium; pH 6.5	7 d	0.45–3.65 mg/g (leaves) 0.33–2.97 mg/g (roots rinsed) 0.49–8.18 mg/g (roots unrinsed)	*Salvinia natans*	[58]
TiO_2NP	275–2398 nm; SSA 50 m^2/g; ζ –20 to –25 mV (est.)	0.01–10 mg/L	Steinburg growth medium; pH 5.5; $CaCO_3$ 166 mg/L	7 d	1–70 mg/kg (whole plant) (est.)	*Lemna minor*	[74]
TiO_2NP	5–10 nm; rhombic and spherical; ζ –33.83 mV	1.8 mg/L	Mesocosm	17 d	424.4 µg/g (root); 64.7 µg/g (stem)	*Oenanthe javanica*	[56]
					54.5 µg/g (whole plant)	*Isoetes japonia*	[56]
TiO_2NP (nanotube)	7–9 nm (width); 2 nm (thick); 6 nm (diameter); tubular; ζ –41.5 mV	1.8 mg/L	Freshwater mesocosm	17 d	73.6 µg/g (root) 5.9 µg/g (stem)	*O. javanica*	[56]
					155.2 µg/g (whole plant)	*I. japonica*	[56]
CuONP	10–15 nm (TEM); 43 nm (SMPS); 6.7 nm (BET); 9 (7 d) ζ –80	1 mg/L	Hoagland's medium; pH 6		800 µg/g (roots) (est.) 700 µg/g (fronds) (est.)	*Landoltia punctata*	[101]

	nm; SSA 141 m^2/g						
CuONP	318 nm	0.68–4.51 g/L	Freshwater culture medium; pH 6.5; IS 12.7 mM	48 h	0.001–0.1 mg/mg (whole plant) (est.)	*Lemna gibba*	[94]
CuONP	97 nm; poly(styrene-co-butyl acrylate) coating; ζ –40 mV	0.25–1.24 g/L	Freshwater culture medium; pH 6.5; IS 12.7 mM	48 h	0.005–0.025 mg/mg (whole plant) (est.)	*L. gibba*	[99]
CuONP	523 nm; ζ –40 mV	0.68–4.51 g/L	Freshwater culture medium; pH 6.5; IS 12.7 mM	48 h	0.006–0.01 mg/mg (whole plant) (est.)	*L. gibba*	[99]
CuONP	38 nm; SSA 12.84 m^2/g; ζ –2.8 mV	0.5–50 mg/L	Hoagland's medium	21 d	14–4057 µg/g (roots) 0.8–17.7 µg/g (shoots)	*Schoenoplectus tabernaemontani*	[75]
CdS	4.3 nm; ζ –9.8 mV	0.5–50 mg/L	Hoagland's medium	21 d	9–1518 µg/g (roots) 0.8–8.7 µg/g (shoots)	*S. tabernaemontani*	[75]
AuNP	65 × 15 nm; rods	7.08×10^8 particles/mL	Estuarine mesocosm; pH 7.7–8.5 (est.); salinity 16.5–18 g/L; DOC 5–12 mg/L (est.)	12 d	3.45 µg/kg (whole plant)	*Spartina alterniflora*	[102]
AuNP	48.3 × 9.8 nm; rods; ζ –53.5 mV	3.42×10^7 particles/mL	Estuarine mesocosm; salinity 20 g/L; pH 8 (est.)	11 d	117 (roots); 4.42 (stems); 1.17 µg/kg (shoots)	*S. alterniflora*	[103]
AuNP (4 nm, 18 nm)	4 nm; 18 nm; spherical; –14.1 mV; ζ –9.73 mV	250 µg/L	Well/borehole water; pH 7.1; DOC 8.56 mg/L; $CaCO_3$ 107 mg/L; conductivity 210 µS/cm	24 h	100 mg/kg (est.); <60 mg/kg (whole plant) (est.)	*Myriophyllum simulans*	[45]
AuNP (4	4 nm; 18 nm; spherical;	250 µg/L	Well/borehole water; pH 7.1;	24 h	120 mg/kg (est.); <60 mg/kg (whole	*Azolla caroliniana*	[45]

nm, 18 nm)	ζ –14.1 mV; ζ –9.73 mV		TOC 8.56 mg/L; $CaCO_3$ 107 mg/L; conductivity 210 µS/cm		plant) (est.)		
AuNP (4 nm, 18 nm)	4 nm; 18 nm; spherical; –14.1 mV; –9.73 mV	250 µg/L	Well/borehole water; pH 7.1; TOC 8.56 mg/L; $CaCO_3$ 107 mg/L; conductivity 210 µs/cm	24 h	40 mg/kg (est.); <60 mg/kg (whole plant) (est.)	*Egeria densa*	[45]
AuNP (4 nm, 18 nm, 30 nm)	8 nm; 17.5 nm; 25 nm; ζ –16.7 mV; ζ –17.8 mV; ζ –23.7 mV	250 µg/L	Well/borehole water; pH 6.8; DOC 0.1 mg/L	24 h	50–150 mg/kg (whole plant) (est.); <50 mg/kg (shoots)	*A. caroliniana*	[42]
AuNP (4 nm, 18 nm, 30 nm)	8 nm; 17.5 nm; 25 nm; ζ –16.7 mV; ζ –17.8 mV; ζ –23.7 mV	250 µg/L	Well/borehole water+DOC; pH 6.8; DOC 2 ± 0.4 mg/L	24 h	<50 mg/kg (whole plant: 4 nm); 50 mg/kg (whole plant: 18 nm, 30 nm) (est.); <50 mg/kg (shoots)	*A. caroliniana*	[42]
AuNP (4 nm, 18 nm, 30 nm)	8 nm; 17.5 nm; 25 ± 7 nm; ζ –16.7 mV; ζ –17.8 mV; ζ –23.7 mV	250 µg/L	Well/borehole water; pH 6.8; DOC 0.1 mg/L	24 h	<50 mg/kg (whole plant); <50 mg/kg (shoots)	*E. densa*	[42]
AuNP (4 nm, 18 nm, 30 nm)	8 nm; 17.5 nm; 25 nm; ζ –16.7 mV; ζ –17.8 mV; ζ –23.7 mV	250 µg/L	Well/borehole water+DOC; pH 6.8; DOC 2 ± 0.4 mg/L	24 h	<50 mg/kg (whole plant); <50 mg/kg (shoots)	*E. densa*	[42]
AuNP (4 nm, 18 nm, 30 nm)	8 nm; 17.5 nm; 25 nm; ζ –16.7 mV; ζ –17.8 mV; ζ –23.7 mV	250 µg/L	Well/borehole water; pH 6.8; DOC 0.1 mg/L	24 h	<50 mg/kg (whole plant); <50 mg/kg (shoots)	*M. simulans*	[42]
AuNP (4	8 nm; 17.5 nm; 25 nm;	250 µg/L	Well/borehole water+DOC; pH	24 h	<50 mg/kg (whole plant);	*M. simulans*	[42]

nm, 18 nm, 30 nm)	ζ –16.7 mV; ζ –17.8 mV; ζ –23.7 mV		6.8; DOC 2 mg/L		<50 mg/kg (shoots)		
AgNP	7.8 nm; gum arabic coating; SSA 100 m^2/g; ζ –49 mV to –44 mV	0.5–10 mg/L	10% Hoagland's medium	72 h	2.81 mg/g (whole plant)	*S. polyrhiza*	[54]
AgNP	240 nm; spherical; SSA 5–10 m^2/g; ζ –31.49 mV	0.01–10 mg/L	Inorganic growth culture medium; pH 6.5; IS 4.25 mM	7 d	7.72–17.75 µg/mg (whole plant)	*L. gibba*	[106]

ENP = engineered nanoparticle; ZnOP = zinc oxide nanoparticle; TiO_2NP = titanium oxide nanoparticle; CuONP = copper oxide nanoparticle; AuNP = gold nanoparticle; AgNP = silver nanoparticle; SSA = specific surface area; TEM = transmission electron microscopy; SMPS = scanning mobility particle sizer; BET = Brunauer–Emmett–Teller method; IS = ionic strength; DOC = dissolved organic carbon; ζ = zeta potential.

large for internalization. Translocation assessment was not done because bioaccumulation analysis was performed on the whole plant [55].

Salvinia natans was exposed to 1 mg/L, 10 mg/L, 20 mg/L, and 50 mg/L ZnONPs as well as 44 mg/L $ZnSO_4$ for 7 d [58]. From ZnONP exposures, Zn accumulation in leaves ranged from 0.45 mg/g to 3.65 mg/g, rinsed roots from 0.33 mg/g to 2.97 mg/g, and unrinsed roots from 0.49 mg/g to 8.18 mg/g. After $ZnSO_4$ exposure, Zn bioaccumulation was 4.28 mg/g in the leaves, 3.82 mg/g in the rinsed roots, and 3.64 mg/g in the unrinsed roots. The results indicated higher bioaccumulation from $ZnSO_4$ than ZnONPs when compared with 50 mg/L ZnONP exposure. In the case of unrinsed roots, bioaccumulation was higher from exposure to ZnONPs than to $ZnSO_4$, and this pointed to the contribution of adsorbed ENPs. Large differences in bioaccumulation between rinsed and unrinsed roots exposed to ZnONPs are indicative of ENP adsorption onto root surfaces. After 7 d, no suspended ZnONPs were detected in suspension of the testing medium because ZnONPs agglomerates sedimented to the bottom of the test vessel. Adsorption to root surfaces also contributed to the removal of ZnONPs in suspension. However, dissolution analysis confirmed the presence of dissolved Zn in the suspension of ZnONPs exposures. Therefore, Zn accumulation was likely the result of the adsorption of ZnONPs and the adsorption and internalization of dissolved Zn forms, with the latter process probably being predominant. Notably, internalization of ZnONPs was unlikely because of the formation of large agglomerates up to 1.6 µm in size, too large for cellular internalization. Zinc content in the leaves and rinsed roots did not differ much, although on average it was higher in the leaves. Such findings can erroneously be interpreted as indicative of active translocation of Zn from the roots to the leaves. This is because *Salvinia* spp. can absorb substances from water through their leaves as well as through their roots [97,98].

The reports on Zn bioaccumulation suggest that the process is directly related to exposure concentration and that the uptake rate for dissolved Zn is higher than that for the nano counterparts. The uptake of ZnONPs is inhibited by transformations such as agglomeration.

TiO_2NPs. Concentration-dependent accumulation of Ti was reported after 7-d exposure of *L. minor* to 0.01 mg/L to 5 mg/L TiO_2NPs [74]. An average of approximately 70 mg/kg whole-plant Ti was recorded at the highest exposure concentration compared with 0.37 mg/kg at the lowest exposure concentration. Electron microscopy analysis detected no internalized TiO_2NPs, pointing to adsorption as the main accumulation mechanism. Formation of larger TiO_2NP agglomerates (100–1000 nm) probably contributed to the lack of TiO_2NP internalization. Translocation was not assessed because bioaccumulation analysis was undertaken for whole plants.

Oenanthe javanica and *Isoetes japonica* were exposed to 1.8 mg/L TiO_2NPs and nanotube TiO_2 (TiO_2NT) forms over 17 d [56] (illumination not reported). Bioaccumulation of Ti was analyzed for the whole body. After 17 d, the total accumulated Ti in *O. javanica* was 489.1 μg/g under TiO_2NP exposure and 78.9 μg/g under TiO_2NT exposure. For *I. japonica*, whole-body Ti was 54.5 μg/g for TiO_2NP exposure and 155.2 μg/g for exposure to TiO_2NT. No explanation was given to account for differences in accumulation of TiO_2NP and TiO_2NT, but the difference may lie in their distinctive morphologies, where orientation of TiO_2NT at sites of contact limited the chance of internalization. Translocation of Ti to the shoot system of *O. javanica* occurred, with Ti accumulation being 424.4 μg/g in the roots and 64.7 μg/g in the shoots under TiO_2NP exposure. In exposures to TiO_2NT, however, Ti concentrations were lower: 73.6 μg/g in the roots and 5.9 μg/g in the shoots.

Because TiO_2NPs compounds are poorly soluble, researchers have considered interaction

and bioaccumulation of TiO_2NPs to be primarily driven by nano forms and have not performed dissolution analyses [56,74]. These studies also highlighted the role of ENP morphology [56] and exposure concentration [74] as factors influencing bioaccumulation by aquatic higher plants.

CuONPs. Perreault et al. [94] compared Cu bioaccumulation in *Lemna gibba* exposed to CuONPs (0.68–4.51 g/L) and $CuSO_4$ (0.004–0.032 g/L) for 48 h. The rate of Cu accumulation was higher from $CuSO_4$ exposure compared with CuONP exposure, and in both regimes it increased with increasing exposure dosage. It was hypothesized that Cu accumulation from CuONP exposure was mainly in dissolved form, as CuONPs agglomerated rapidly in suspension. The same research group also investigated the influence of coating, concentration, and Cu form (particulate or dissolved) on the bioaccumulation of Cu by *L. gibba* [99]. *Lemna gibba* was exposed to noncoated CuONPs, styrene-co-butyl acrylate–coated CuONPs, and $CuSO_4$ for 48 h. In all exposures, whole-body Cu increased with increasing exposure concentration. Furthermore, bioaccumulation concentration was established in descending order as $CuSO_4$ > coated CuONPs > uncoated CuONPs. These findings [100] suggested that dissolved Cu forms were rapidly accumulated compared with nano counterparts. Dissolution of both CuONPs forms was largely negligible, which pointed to accumulation arising from the particulate forms.

The coating of CuONPs improved their uptake because of enhanced stability (retention of smaller sizes as coating inhibited aggregation) compared with uncoated forms that largely agglomerated (probably exhibiting a higher settling rate), which limited their uptake. Polymer-coated CuONPs were more toxic to microalgal species compared with uncoated CuONPs [100], chiefly because the smaller coated CuONPs were more able to interact with and penetrate the cells than uncoated CuONPs. Similarly, higher uptake of smaller-sized AuNPs by aquatic higher plants as a result of natural organic matter steric stabilization has also been reported [45]. Thus,

the surface coating of ENPs appears to influence their accumulation by aquatic plants, although this is subject to the activity of other water quality parameters. Studies on the exposure of *S. tabernaemontani* to CuONPs (0.5 mg/L, 5 mg/L, and 50 mg/L) showed that Cu accumulation was dependent on both exposure concentration and duration [75]. After 21 d, at 50 mg/L, the roots accumulated Cu to more than 4000 µg/g and the shoots less than 20 µg/g, an indication of limited translocation from the roots to shoots. Internalized CuONPs were detected in the epidermis and inside cells; hence, Cu bioaccumulation probably resulted from adsorption and internalization of both the CuONP particulates and dissolved Cu species.

Shi et al. [101] reported that *Landoltia punctata* accumulated approximately 700 µg/g Cu in the fronds and 800 µg/g Cu in the roots after exposure to 1 mg/L CuONPs for 14 d. In the same study, the plants were exposed to 0.2 mg/L or 0.6 mg/L dissolved Cu ($CuCl_2$). Bioaccumulation of Cu was approximately <100 µg/g (fronds) and 300 µg/g (roots) from the 0.2-mg/L exposure, whereas the 0.6-mg/L exposure yielded 500 µg/g (fronds) and 700 µg/g (roots). Although the findings appear to suggest a higher assimilation rate of CuONPs, the exposure concentrations of CuONPs and $CuCl_2$ differed, making comparisons difficult. Bioaccumulation from CuONP exposures probably resulted from uptake of soluble Cu (based on dissolution findings), adsorption of CuONPs, and maybe their internalization. The findings further suggested transportation of Cu^{+}/Cu^{2+}/Cux/CuONPs from roots to leaves, but there is need for caution, as leaves of this plant type are capable of absorbing nutrients from the surrounding environment.

Overall, the uptake of dissolved Cu appears to be the main driver of CuONP bioaccumulation, based on the findings of Perreault et al. [94,99]. Moreover, it can also result from the accumulation of both dissolved and particulate Cu forms [75]. Interestingly, the

findings of Shi et al. [101] differ from those of Perreault et al. [94,99]. This is because accumulation of CuONPs was reported to be higher than $CuCl_2$ exposures in Shi et al. [103]. However, the exposure concentrations of $CuCl_2$ (0.2 mg/L, 0.6 mg/L) and CuONPs (1 mg/L) differed [101], which may have led to underestimation of soluble Cu accumulation potential and prohibits any meaningful comparison between accumulation of soluble Cu and CuONPs.

AuNPs. Ferry et al. [102] demonstrated that *Spartina alterniflora* exposed to AuNP rods for 12 d in an estuarine mesocosm had a whole-plant Au concentration of 3.45 μg/kg. The observed bioaccumulation was ascribed to adsorption of the insoluble AuNP rods, which formed agglomerates that were deemed too large for internalization. However, much higher Au accumulation by *S. alterniflora* occurred during 11-d exposure to AuNP rods under similar estuarine mesocosm conditions [103]. Bioaccumulation of Au was 117 μg/kg in roots (more than 30 times that reported by Ferry et al. [102]), 4.42 μg/kg in stems, and 11.3 μg/kg in aerial parts. Exposure concentrations were 7.08×10^8 particles/mL in Ferry et al. [102] and 3.42×10^7 particles/mL in Burns et al. [103]; the cause of the much higher bioaccumulation is unclear.

The higher Au accumulation in the roots was associated with adherence of sediment particles to the roots, even though the roots were washed to remove sediment particles [103]. Bioaccumulation analysis also indicated probable active translocation of Au from roots as sites of uptake through stems, where accumulation was less, to aerial parts, where deposition was more than double that in the stems. As a member of the Poaceae family, absorption of nutrients in *S. alterniflora* is primarily a function of the roots because a thick cuticle to reduce water loss in stems and shoots inhibits this function [45]. Bioaccumulation rates of AuNPs may be dependent on ENP size and the plant species [42,45]. For example, higher Au accumulation was observed from 4-nm AuNPs compared with 18-nm AuNPs across all plant species [45]. *Azolla*

caroliniana accumulated in excess of 120 mg/kg Au from 4-nm AuNPs exposure and less than 60 mg/kg from 18-nm AuNPs exposure. Similar trends were observed in other experiments, where less Au bioaccumulation was found in plants exposed to 30-nm AuNPs than to 4-nm or 18-nm AuNPs [42]. Such AuNPs accumulation patterns were ascribed to relatively higher internalization rates of smaller AuNPs particulate forms, for instance, by *M. simulans* and *A. caroliniana* [45].

Conversely, no AuNPs internalization was found in *E. densa*, so the observed bioaccumulation was wholly attributed to adsorption of ENPs because dissolution was insufficient for appreciable internalization of soluble Au. In both studies [42,45], Au accumulation was highest in *A. caroliniana*, moderate in *M. simulans*, and lowest in *E. densa*. The interspecies differences were attributed to varying morphological and physiological characteristics between the species. Moreover, bioaccumulation of Au was found to be influenced by water chemistry (namely, natural organic matter concentration) [42]. Addition of natural organic matter inhibited accumulation caused by the formation of AuNP–DOC complexes that were larger than the cell wall pores, resulting in reduced potential for AuNP uptake. Although no uptake was observed because of AuNPs–DOC complex formation, AuNPs stability was enhanced, an effect that could extend their persistence in the environment.

Generally, poor solubility of AuNPs suggests that their bioaccumulation by aquatic higher plants is mainly through accumulation of nano particulates. This means it is mostly influenced by characteristics of AuNPs and exposure media properties. For instance, the role of bioaccessible size is evident in reports from Glenn and Klaine [42] and Glenn et al. [45] but varies between plant species and physicochemical conditions of the exposure medium. The role of roots in nutrient absorption also facilitates accumulation of AuNPs because the Au content in

roots was high. Depending on the plant species, AuNPs can be translocated to aerial tissues as well.

Silver nanoparticles. Spirodela polyrhiza was exposed to silver nanoparticles (AgNPs) and $AgNO_3$ (0.5–10 mg/L) for 72 h in a study by Jiang et al. [54]. The bioaccumulation of Ag from both Ag forms was dependent on exposure concentration and was much higher in plants exposed to $AgNO_3$. After 72 h at 10 mg/L exposure dosage, the average Ag bioaccumulation from AgNPs was below 4 mg/g but above 10 mg/g from $AgNO_3$ [54]. The findings suggest that bioaccumulation of soluble Ag was rapid compared with that of AgNPs, similar to other ENPs (see the sections *ZnONPs* and *CuONPs*, above). Other reports on Ag have associated interactions with aquatic biota with the formation of soluble Ag species [104,105], so adding dissolution analysis to the procedure of Jiang et al. [54] would help elucidate probable mechanisms for AgNP bioaccumulation. Higher accumulation of Ag from $AgNO_3$ exposures may be linked to its higher solubility, thus enhancing internalization, unlike AgNPs, which have low solubility [44,106]. This hypothesis appears plausible based on the generally low solubility of AgNPs [44,106,107]. No translocation data are available because whole-plant Ag accumulation was undertaken in the studies of Jiang et al. [54].

Lemna gibba exposed to AgNPs for 7 d accumulated Ag dependent on exposure concentration, ranging from 7.72 µg/mg to 17.5 µg/mg under exposure to AgNPs concentrations of 0.01 mg/L to 10 mg/L [106]. Bioaccumulation was mainly associated with internalized AgNPs, since the plants were washed with chelating ethylenediaminetetraacetic acid (EDTA) and dissolution was approximately1% of nominal dose. However, no plant cross sections were examined with electron microscopy to assess internalization of AgNPs. Based on the AgNPs hydrodynamic size distribution (159–447 nm), the agglomerates appeared too large for Ag

bioaccumulation to be largely attributed to AgNPs internalization. Therefore, it is likely that the adsorbed AgNPs and dissolved Ag forms accounted for the reported bioaccumulation, since no evidence was presented suggesting complete removal of adsorbed AgNPs/soluble Ag after washing with EDTA. Thus, the analysis of plant cross sections with electron microscopy would have offered useful insights into the hypothesis of AgNP internalization suggested by Hund-Rinke et al. [13].

The reports on Ag bioaccumulation following AgNP exposure suggest that the process is dependent on exposure concentration and that accumulation of dissolved Ag forms is rapid relative to nano counterparts. Other than the release of soluble forms, other mechanisms for AgNP bioaccumulation are yet to be explored in detail. For example, adsorption and internalization of AgNPs are yet to be reported, including the ENP characteristics that can influence such bioaccumulation mechanisms. Bioaccumulation of AgNPs is likely to be size-dependent, being greater at smaller sizes as a result of raised potential for dissolution, internalization, and adsorption.

CdS QDs. The bioaccumulation of Cd by *S. tabernaemontani* depended on exposure duration and concentration in plant roots and shoots following 21-d exposure to 0.5 mg/L, 5 mg/L, and 50 mg/L CdS QDs [75]. Bioaccumulation of Cd in the roots (~1500 µg/g) was 190-fold higher than that in the shoots (~8 µg/g), which indicated limited translocation from roots to shoots. Both adsorption and internalization of CdS QDs were evidently accumulation drivers, with the former being dominant because of the association of nanoparticles with the roots.

Summary: Bioaccumulation and translocation. Accumulation of ENPs by aquatic higher plants is complex, with environmental parameters and ENP transformations interacting to influence the uptake process (Tables 1 and 2). Reports of ENP internalization were few (Table

1), probably because of the difficulty associated with tissue sample preparation and the specialized analytical equipment required. Differentiating between internalization and adsorption of ENPs provides useful information for hazard and bioavailability assessment exercises. For trophic transfer and phytoextraction evaluation, however, such discrimination is of limited value. Total metal bioaccumulation has been utilized predominantly as an indicator of ENP accumulation (Table 2), most likely because of the simpler analytical protocol and more accessible analytical equipment required, such as inductively coupled plasma optical emission spectroscopy or inductively coupled plasma mass spectroscopy. Generally, bioaccumulation depended on exposure concentration and ENP size, influenced by ENP surface chemistry/coating. Bioaccumulation of soluble metal forms was higher than that of nano particulates. Furthermore, adsorption of both the dissolved and nano metallic derivatives contributed notably to bioaccumulation. The bioaccumulation of bulk-scale metals by aquatic biota is apparently related to exposure concentration, but the bioconcentration factor is inversely related to exposure concentration for chronic exposures [108]. Therefore, metal bioaccumulation resulting from the metal-based ENPs reviewed in the present study is in agreement with trends for bulk-scale counterparts. Predictions about the predominant driver of bioaccumulation between metallic particles and soluble metallic forms were mostly founded on dissolution analysis of the exposure water. The solubility of ENPs appears to influence bioaccumulation, as enhanced bioaccumulation tended to be associated with higher solubility, suggesting lower uptake potential for ENPs relative to soluble metal derivatives.

TOXICITY EFFECTS

A growing body of scientific literature describes the toxicity of different classes of ENPs,

such as metals [44,54,104,107], metal oxides [44,55,58,109], and quantum dots [75], to aquatic higher plants. For simplicity, in the present review, the toxicological endpoints are categorized as subcellular (oxidative stress and damage), photosynthetic (chlorophyll pigments and photosynthetic activity), and growth (biomass and growth rate) effects.

Subcellular

The subcellular category of effects consists of endpoints such as activity of antioxidants, oxidative damage, and protein content. Findings on subcellular effects of metal-based ENPs to aquatic higher plants and relative exposure conditions are summarized in Table 3.

CuONPs. A 48-h exposure of *L. gibba* to $CuSO_4$ (0.004–0.032 g/L), polymer-coated CuONPs (0.25–1.24 g/L), and bare CuONPs (0.68–4.51 g/L) inhibited esterase enzyme activity and enhanced generation of reactive oxygen species (ROS). The effects were dependent on exposure concentration [99]. The ROS generation per viable biomass was in the order $CuSO_4$ > coated CuONPs > uncoated CuONPs. However, ROS formation based on soluble Cu fractions and Cu bioaccumulation was coated CuONPs > uncoated CuONPs > $CuSO_4$. The findings suggested that for CuONP ROS generation, the basis was nano driven compared with soluble Cu, because the latter was less oxidative, and such findings were attributed to rapid uptake of the coated and more stable CuONPs. On the activity of esterase enzyme, the effect was $CuSO_4$ > uncoated CuONPs > coated CuONPs. The findings for the esterase enzyme indicated that soluble Cu was highly toxic to the nano counterparts. The investigation [99] suggested that toxicity of CuONPs is dependent on the endpoint being assessed and solubility potential. Further studies will improve our understanding of the difference in toxicological potency between CuONPs and soluble Cu.

Table 3. Summary of subcellular effects in aquatic higher plants exposed to metal-based ENPs

ENP	ENP characteristics	Exposure water	Exposure concentration	Duration	Endpoint	Effect/response	Plant	Ref.
CuONP	523 nm; ζ –40 mV	Freshwater culture medium; pH 6.5; IS 12.7 mM	0.7–4.5 g/L	48 h	Esterase	Decreased	*Lemna gibba*	[99]
					ROS	Increased		
CuONP	97 nm; poly(styrene-co-butyl acrylate) coating; ζ –40 mV	Freshwater culture medium; pH 6.5; IS 12.7 mM	0.3–1.2 g/L	48 h	Esterase	Decreased	*L. gibba*	[99]
					ROS	Increased		
TiO_2NP	10 nm; ζ –15 mV to 25 mV (est.); SSA 120 m^2/g	10% Steinberg medium; irradiance 72 µmol/m^2/s	10–2000 mg/L	7 d	POD	Activated	*Lemna minor*	[109]
					CAT	Activated		
					SOD	Activated then inhibited		
					MDA	Increased		
ZnONP	25 nm; uncoated; 90 m^2/g; spherical	Hoagland's medium; pH 6.5	1–50 mg/L	96 h	CAT	Activated (50 mg/L)	*Spirodela polyrhiza*	[55]
					POD	Inhibited (50 mg/L)		
					SOD	Activated (≥10 mg/L)		
					Na^+K^+ATPase	Uniform		
ZnONP	25 nm; uncoated; 90 m^2/g; 1–10 mg/L	OECD growth medium; pH 6.5	1–50 mg/L	7 d	SOD	Activated (50 mg/L)	*Salvinia natans*	[58]
					CAT	Activated (50 mg/L)		
					POD	Inhibited (50 mg/L)		
AgNP	240 nm; spherical; SSA	Inorganic growth	0.01–10 mg/L	7 d	Cell viability	Reduced from 0.1 mg/L	*L. gibba*	[106]

	5–10 m^2/g; ζ –31.49 ± 2.16 mV	culture medium; pH 6.5; IS 4.25 mM			ROS formation	Increased from 1 mg/L		
ZnONP	326–1350 nm; ζ –4.9 mV to 11 mV; SSA 11.4 m^2/g; spheres; polydispersed morphology	Hoagland's medium	0.01–1000 mg/L	14 d	ROS/RNS H_2O_2 TAC SOD	Increased then stabilized (4 d) Increased (14 d) Uniform (4 d) then increased at highest exposure dose (14 d) Increased at lowest exposure dose (4 d) Inhibited (14 d); only activated at highest dosage (14 d)	*Spirodela punctata*	[44]
AgNP	352–1313 nm; ζ –3.6 mV to 11.6 mV; SSA 3.4 m^2/g; polydispersed morphology	Hoagland's medium	0.01–1000 mg/L	14 d	ROS/RNS H_2O_2 TAC SOD	Uniform (4-14 d) Increased Uniform Inhibited and activated (4 d); inhibited (14 d)	*S. punctata*	[44]
AgNP	7.8 nm; gum arabic coating; SSA 100 m^2/g; ζ –49 mV to –44 mV	10% Hoagland's medium	0.5–10 mg/L	72 h	Nitrate-nitrogen Phosphate-phosphorus Carbohydrate Proline	Reduced (≥5 mg/L) Uniform Uniform (5 mg/L) Increased (≥5m g/L)	*S. polyrhiza*	[54]

AgNP	7.8 nm; gum arabic coating; SSA 100 m^2/g; ζ –49 mV to –44 mV; spherical	10% Hoagland's medium	0.5–10 mg/L	72 h	ROS content	Increased (≥1 mg/L)	*S. polyrhiza*	[107]
					SOD	Activated		
					POD	Activated (≥5 mg/L)		
					CAT	Activated (5 mg/L)		
					Protein content	Increased (1 mg/L, 5 mg/L)		
					MDA	Increased (5 mg/L)		
					GSH	Increased (5 mg/L)		
AgNP	22.9 nm; PVP coating; spherical	10% Hoagland's medium	10 mg/L	72 h	ROS content	Increase	*S. polyrhiza*	[107]
					SOD	Increase		
					POD	Increase		
					CAT	No significant effect		
					Protein content	Increase		
					MDA	No significant effect		
					GSH	Increase		

ENP = engineered nanoparticle; CuONP = copper oxide nanoparticle; TiO_2NP = titanium oxide nanoparticle; ZnOP = zinc oxide nanoparticle; AgNP = silver nanoparticle; IS = ionic strength; ROS = reactive oxygen species; SSA = specific surface area; POD = peroxidase; CAT = catalase; SOD = superoxide dismutase; MDA = malondialdehyde; OECD = Organisation for Economic Co-operation and Development; GSH = glutathione; RNS = reactive nitrogen species; TAC = total antioxidative capacity; PVP = polyvinylpyrrolidone; ζ = zeta potential

TiO_2NPs. Song et al. [109] investigated the induction of oxidative stress to *L. minor* following exposure to bulk and nano forms of TiO_2 (10–2000 mg/L). There was activation of peroxidase (POD), catalase (CAT), and malondialdehyde (MDA) in plants exposed to TiO_2NPs across exposure concentrations. Bulk TiO_2 was generally toxic at high exposure concentrations; for example, it only activated POD and superoxide dismutase (SOD) at 2 g/L and CAT at 1 g/L to 2 g/L. The results pointed to higher toxicity of TiO_2NPs compared with bulk counterparts, a size-dependent phenomenon. It can be assumed that there was better uptake of TiO_2NPs but also that bulk TiO_2 rapidly settled out of suspension because of its size. The investigators did not account for possible differences between the toxicity of TiO_2NPs and bulk TiO_2. However, it also is plausible that photo-activation of TiO_2NPs was enhanced compared with larger counterparts.

ZnONPs. The activities of CAT, POD, SOD, and sodium/potassium adenosine 5′-triphosphatase (Na^+K^+-ATPase) were assayed in *S. polyrhiza* following 96-h exposure to ZnONPs (1–50 mg/L) and $ZnSO_4$ (3.5 mg/L) [55]. All endpoints were significantly altered by $ZnSO_4$; it stimulated CAT and SOD but inhibited POD and Na^+K^+-ATPase. For ZnONPs, Na^+K^+-ATPase was insignificantly influenced, and SOD activity increased by ≥10 mg/L, whereas both CAT and POD were only significantly stimulated at the highest exposure concentration. Both SOD and CAT activities were stimulated by 10 mg/L to 50 mg/L of ZnONPs as well as exposure to $ZnSO_4$. Conversely, $ZnSO_4$ inhibited the POD and Na^+K^+ATPase, but ZnONPs only inhibited POD at the highest concentration. When comparing similar exposure concentrations, dissolved Zn ($ZnSO_4$) was more toxic than ZnONPs. Because of the agglomeration of ZnONPs, the dissolved Zn derivatives were postulated to be the underlying cause of the observed toxicological effects following ZnONP exposures. Immediate

agglomeration (average of ~0.3 µm) at 0 h occurred, leading to sedimentation. No ZnONPs were detected in suspension after 12 h. Similarly, in a study by Hu et al. [58], dissolved Zn was raised as the dominant cause of toxicity to *S. natans* exposed to ZnONPs (1–50 mg/L) and $ZnSO_4$ (44 mg/L) for 7 d. Zinc oxide nanoparticles activated SOD at 10 mg/L to 50 mg/L and CAT at 50 mg/L, inhibited POD at 50 mg/L, and were not toxic to Na^+K^+-ATPase. Also, $ZnSO_4$ activated SOD and CAT, but inhibited POD and Na^+K^+-ATPase [58].

Thwala et al. [44] exposed *Spirodela punctata* to ZnONPs (0.01–1000 mg/L) for 14 d, and the results revealed induction of various forms of oxidative imbalances. The observed effects exhibited both temporal and dose dependence. For example, the production of reactive oxygen and nitrogen species (ROS/RNS) evaluated by the 2′,7′-dichlorodihydrofluorescein method at the highest exposure concentration was below 1.5 nM after 4 d but reached 175 nM after 14 d. Furthermore, minimum ROS/RNS production of approximately 25 nM was observed at 0.01 mg/L ZnONPs and increased to 175 nM at 1000 mg/L ZnONPs, indicating that free radical production was dose-dependent. Similarly, hydrogen peroxide (H_2O_2) and total antioxidant capacity were much higher after 14 d than after 4 d of exposure. However, similar SOD activity was observed at the highest exposure concentration regardless of exposure duration. The effects were associated with the dissolved Zn based on the dissolution data: at the highest exposure concentration, the dissolved Zn concentration was 12 mg/L after 4 d and 13 mg/L after 14 d, which may account for the similarity in SOD activity irrespective of the exposure period. The nano counterparts underwent rapid agglomeration, reaching sizes of up to 1350 nm, and settled out of suspension.

AgNPs. Jiang et al. [54] reported that *Spirodela punctata* experienced significant reduction of total nitrate-nitrogen, phosphate-phosphorus, and carbohydrate after exposure to 0.5

mg/L to 10 mg/L of AgNPs and $AgNO_3$. The effects were exposure concentration-dependent. Similarly, proline production, an indicator of stress, increased with increasing exposure concentration. The Silver nitrate had greater toxic effects than AgNPs, suggesting that the toxicological potency of dissolved Ag is higher than that of the nano forms. Dissolution analysis would be required to accurately establish whether the underlying driver of AgNP toxicity was dissolved or nano Ag. However, AgNPs exhibit slow dissolution [44,106,107]; therefore, their toxicity was probably a nano effect. Free radical production in *S. punctata* was AgNP dose-dependent [44] and declined at higher concentrations because of the reduction in biomass, with 100% mortality at the highest exposure concentration. The observed SOD activity inhibition attributable to AgNPs was postulated to be a result of protein denaturation after oxidative damage. The dissolution of AgNPs was virtually negligible (below detection after 14 d at the highest concentration), so dissolved Ag species had very little influence on the observed toxicity [44]. *Lemna gibba* exposed to 0.01 mg/L to 10 mg/L AgNPs for 7 d [106] showed free radical activity assayed by 2′,7′-dichlorodihydrofluorescein fluorescence, which increased with increasing exposure concentration. Cell viability was also affected by AgNPs, where the percentage of viable cells initially increased at the lowest dosage but significantly decreased at all other exposure dosages. Based on low solubility of AgNPs, the dissolution of internalized AgNPs was most likely the main driver of the toxic effects [106].

Jiang et al. [107] reported size-dependent toxicity of AgNPs on *S. polyrhiza* following exposure to average 6-nm AgNPs (0.5–10 mg/L), 20-nm AgNPs (10 mg/L), and >1-µm Ag (10 mg/L) for 72 h. The endpoints assayed were ROS, SOD, CAT, POD, MDA, reduced glutathione (GSH), and protein content. The ROS content was raised by 6-nm AgNPs (≥0.5 mg/L) and 20-nm AgNPs but not by bulk Ag. All AgNPs forms increased SOD activity, but this was not the

case with bulk Ag. Catalase activity and MDA content were raised only by 5 mg/L with exposure to 6-nm AgNPs. Exposure to 5 mg/L to 10 mg/L of 6-nm AgNPs and 20-m AgNPs increased POD activity. Protein content was elevated by 1 mg/L to 5 mg/L of both the 6-nm and 20-nm AgNPs. Lastly, the GSH content was increased by 6-nm AgNPs (≥1 mg/L), 20-nm AgNPs, and bulk Ag. Therefore, bulk Ag was toxic to GSH only and not to any of the other endpoints. Dissolution of AgNPs was slower than that of bulk Ag, which suggested that AgNPs toxicity was mainly nano driven. The contradiction between the 2 studies [54,107] results from the fact that $AgNO_3$ was used in the former [54], whereas micron-sized Ag was used in the latter [107]; hence, the Ag derivatives were chemically different.

Photosynthetic effects

Grouped under photosynthetic effects were endpoints associated with the functioning of the photosynthetic pathway. Table 4 provides a summary of findings on the photosynthetic effects of metal-based ENPs to aquatic higher plants.

CuONPs. The effects of CuONPs (0.7–4.5 g/L) and $CuSO_4$ (0.004–0.032 g/L) on the photosynthetic system of *L. gibba* were reported by Perreault et al. [94]. Both CuONPs and $CuSO_4$ inhibited photosystem II activity, and the toxicity of the Cu salt was greater than that of its nano counterparts. Various endpoints were assayed to assess the effects on the energy fluxes in the photosynthetic membrane. Both Cu forms reduced the number of active photosystem II reaction centers per chlorophyll unit and further affected photosystem II yield similarly. The toxicity of CuONPs was mainly associated with the release of dissolved Cu forms. *Lemna gibba* exposed to bare CuONPs (0.68–4.51 g/L), polymer-coated CuONPs (0.25–1.24 g/L), and $CuSO_4$ (0.004–0.032 g/L) [100] had photosystem II inhibited in all exposures, and toxicity was shown to

Table 4. Summary findings of photosynthetic effects in aquatic higher plants exposed to metal-based ENPs

ENP	ENP characteristics	Exposure water	Exposure concentration	Duration	End point	Effect/response	Plant	Ref.
CuONP	109–523 nm	Freshwater culture medium; pH 6.5; IS 12.7 mM	0.68–4.5 g/L	48 h	PSII activity PSII yield	Decreased Decreased	*Lemna gibba*	[94]
CuONP	523 nm; ζ –40 mV	Freshwater culture medium; pH 6.5; IS 12.7 mM	0.7–4.5 g/L	48 h	PSII performance index	Inhibited	*L. gibba*	[99]
CuONP	97 nm; poly(styrene-co-butyl acrylate) coating; ζ –40 mV	Freshwater culture medium; pH 6.5; IS 12.7 mM	0.3–1.2 g/L	48 h	PSII performance index	Inhibited	*L. gibba*	[99]
CuONP	10–15 nm (TEM); 43 nm (SMPS); 6.7 nm (BET); 9 (7 d) –80 nm; SSA 141 m^2/g	Hoagland's medium; pH 6	1 mg/L	14 d	Chl *a* Chl *b* Chl *a*+Chl *b*	Decreased Decreased Decreased	*Landoltia punctata*	[101]
TiO_2NP	10 nm; ζ –15 mV to –25 mV (est.)	10% Steinberg medium; pH 6.5; irradiance 72 µmol/m^2/s	10–2000 mg/L	7 d	Chlorophyll content	Increased (≤200 mg/L)	*Lemna minor*	[109]
TiO_2NP	275–2398 nm; SSA 50 m^2/g	Steinburg growth medium; pH 5.5;	0.01–10 mg/L	7 d	Chl *a*	No significant effects	*L. minor*	[74]

		$CaCO_3$ 166 mg/L; irradiance 5000 lx						
Al_2O_3NP	9.01 nm (TEM); 165–189 nm (NTA); SSA 200 m^2/g; spherical to void; ζ 5.3 mV	50% Hutner's medium; pH 5.3	10–1000 mg/L	7 d	PSII yield Photochemical quench Non-photo quench	Increased (100 mg/L) Increased (100 mg/L) No significant effects	*L. minor*	[111]
ZnONP	25 nm; SSA 90 m^2/g	Hoagland's medium; pH 6.5	1–50 mg/L	96 h	Chl:pheophytin	Reduced (50 mg/L)	*Spirodela polyrhiza*	[55]
ZnONP	25 nm; SSA 90 m^2/g	Hoagland's medium; pH 6.5	1–50 mg/L	7 d	Chl *a* Chl *b* Carotenoid	Increased (50 mg/L) No effects Increased (50 mg/L)	*Salvinia natans*	[58]
AgNP	7.8 nm; gum arabic coating; SSA 100 m^2/g; ζ –49 mV to -44 mV	10% Hoagland's medium	0.5–10 mg/L	72 h	Chl *a* Chl *a*/*b* Chl total Photochemical efficiency	Decreased Decreased (≥5 mg/L) Decreased Decreased	*S. polyrhiza*	[54]

ENP = engineered nanoparticle; CuONP = copper oxide nanoparticle; TiO_2NP = titanium oxide nanoparticle; Al_2O_3NP = aluminium oxide nanoparticle; ZnOP = zinc oxide nanoparticle; AgNP = silver nanoparticle; PSII = photosynthetic system II; TEM = transmission electron microscopy; SMPS = scanning mobility particle sizer; BET = Brunauer–Emmett–Teller method; SSA = specific surface area; NTA = nanoparticle tracking analysis; ζ = zeta potential.

be exposure concentration-dependent. Soluble Cu was more toxic than either nano form, and the bare CuONPs were the less toxic nano form. The findings were attributed to a rapid uptake rate of soluble Cu and to coated CuONPs being more stable than uncoated CuONPs, which were observed to agglomerate rapidly.

Shi et al. [101] exposed *L. punctata* to CuONPs (1 mg/L) and $CuCl_2$ (0.2 mg/L and 0.6 mg/L) for 14 d. The Cu salt reduced chlorophyll content (*a*, *b*, *a*+*b*) in a concentration-dependent manner. It was unclear which of the 2 Cu derivatives was more toxic, since the exposure concentrations differed. The solubility of CuONPs was 0.16 mg/L, which suggested that its toxicity was mainly nano driven. From the $CuCl_2$ exposures, the dissolved Cu was determined to be 0.2 mg/L and 0.6 mg/L. Although Cu is an essential element in plant physiology, when in excess it inhibits photosynthesis, especially photosystem II [110].

TiO_2NPs. Exposure of *L. minor* to TiO_2NPs (10–2000 mg/L) caused an increase of chlorophyll content in a dose-dependent trend, but no effects were observed following exposure to bulk-TiO_2 [109]. Such findings were suggestive of size-influenced toxicity of TiO_2. The 200 mg/L to 2000 mg/L concentrations of TiO_2NPs significantly increased chlorophyll content. The effect on TiO_2NPs of increasing chlorophyll content appeared to enhance photosynthesis, whereas an inhibition effect would generally be expected. This was puzzling because growth inhibition was observed at similar exposure concentrations. The reason for such observations was not investigated. The chlorophyll content in *L. minor* exposed to 0.01 mg/L to 5 mg/L TiO_2NPs remained similar to that of control samples [74]. The lack of negative effects on chlorophyll *a* was attributed to the lack of TiO_2NP internalization, suggesting it was not bioavailable to the plants. In summary, both studies [74,109] appear to suggest that the negative effect on chlorophyll *a* in *L. minor* would occur only at very high concentrations, which are not

environmentally realistic.

Aluminium oxide nanoparticles. Aluminium oxide nanoparticles (Al_2O_3NPs) increased the photosynthetic efficiency of *L. minor* [111], but the effect was not exposure concentration–dependent. The photosynthetic efficiency measured as photosystem II quantum yield and photochemical quenching increased as the exposure concentrations increased and was more significant at higher exposure concentrations. However, nonphotochemical quenching was least at higher concentrations.

ZnONPs. Spirodela polyrhiza was exposed to ZnONPs (1–50 mg/L) and $ZnSO_4$ (3.5 mg/L) for 96 h [55]. Only the 50 mg/L ZnONP exposure reduced the chlorophyll *a* to pheophytin ratio, whereas $ZnSO_4$ was inhibitive at 3.5 mg/L. Thus, soluble Zn ($ZnSO_4$) was highly toxic compared to the nano derivatives. The toxicity of ZnONPs was associated with its dissolution because it underwent aggregation under the exposure conditions. Hu et al. [58] exposed *S. natans* to 1 mg/L to 50 mg/L ZnONPs and 44 mg/L $ZnSO_4$. Assay results for chlorophyll *a*, *b*, and carotenoid indicated that $ZnSO_4$ inhibited all the endpoints; however, ZnONPs only inhibited the chlorophylls at the highest exposure concentration. Similar to the findings of Hu et al. [55], $ZnSO_4$ was more toxic than ZnONPs to *S. polyrhiza* when compared at similar exposure concentrations. Therefore, the 2 studies [55,58] collectively point to dissolution driven toxicity of ZnONPs.

AgNPs. Exposure of *S. polyrhiza* to AgNPs and $AgNO_3$ (0.5–10 mg/L) for 96 h reduced chlorophyll *a*, chlorophyll *a*/chlorophyll *b*, and photochemical efficiency ratio. The effect was exposure concentration–dependent [54]. Although $AgNO_3$ seemed relatively more toxic, the authors argued that the toxicity of the 2 Ag forms was generally similar; however, sensitivity varied between toxicity endpoints. Following low Ag bioaccumulation in AgNP exposures [54],

it can be hypothesized that if uptake of AgNPs was increased likewise, the toxicity of AgNPs would likely be higher than that of $AgNO_3$ based on mass/volume exposure concentrations. This case further indicates the need for more detailed information on the uptake kinetics of ENPs by aquatic higher plants. Future studies need to consider whether linkages exist between the toxicity effects and accumulation of ENPs.

Growth effects

The effects on plant growth parameters are presented in the present section. Table 5 summarizes findings from investigations of metal-based effects on aquatic higher plants.

CuONPs. Lemna gibba exposed to $CuSO_4$, bare CuONPs, and polymer-coated CuONPs for 48 h experienced growth inhibition from all the Cu exposures [99]. The toxicity was ranked as $CuSO_4$ > polymer-coated CuONPs > bare CuONPs, where the latter caused the least growth inhibition. The results indicated higher toxicity of soluble Cu compared with nano particulates, and the former demonstrated a higher accumulation rate. The polymer-coated CuONPs were more inhibiting compared with bare CuONPs, and the effect was suggested to be the result of polymer alteration of cellular interaction and higher stability, which in turn enhanced uptake and toxicity. Also in the findings of Perreault et al. [94], soluble Cu ($CuSO_4$) was more growth-inhibiting than CuONPs toward *L. gibba* following a 48-h exposure. The toxicity of CuONPs was attributed to the release of soluble Cu, considering that CuONPs rapidly agglomerated and settled at the bottom of the test vessel at a higher rate.

In another study, the growth effects of $CuCl_2$, CuONPs, and bulk CuO in *L. punctata* were studied for 96 h [101]. Frond numbers were most reduced by the Cu salt and CuONPs, and bulk CuO was the least toxic form. Bulk CuO was less toxic than CuONPs, as the latter was

Table 5. Summary findings on growth effects in aquatic higher plants exposed to metal-based ENPs

ENP	ENP characteristics	Exposure water	Exposure concentration	Duration	End point	Effect/response	Plant	Ref.
CuONP	38 nm; SSA 12.84 m^2/g; ζ –2.8 mV	25% Hoagland's medium	0.5–50 mg/L	21 d	Biomass	No significant effects	*Schoenoplectus tabernaemontani*	[75]
CdS QDs	4.3 nm; –9.8 mV	25% Hoagland's medium	0.5–50 mg/L	21 d	Biomass	Reduction ≥5 mg/L	*S. tabernaemontani*	[75]
CuONP	109–523 nm	Freshwater culture medium; pH 6.5; IS 12.7 M	0.4–4.5 g/L	48 h	Growth rate	Growth reduction >0.1 Cu g/L	*Lemna gibba*	[94]
CuONP	97 nm; poly(styrene-co-butyl acrylate) coating; ζ –40 mV	Freshwater culture medium; pH 6.5; IS 12.7 M	0.3–1.2 g/L	48 h	Growth rate	Inhibited	*L. gibba*	[99]
CuONP	523 nm; ζ –40 mV	Freshwater culture medium; pH 6.5; IS 12.7 M	0.7–4.5 g/L	48 h	Growth rate	Inhibited	*L. gibba*	[99]
CuONP	10–15 nm (TEM); 43 nm (SMPS); 6.7 nm (BET); 9 (7 d) 80 nm; SSA 141 m^2/g	Hoagland's medium; pH 6.5 ± 0.2	0.0158–4 mg/L	96 h	Frond number	Reduced	*Landoltia punctata*	[101]
			1 mg/L	9 d	Frond number	Reduced	*L. punctata*	[101]

			1 mg/L	9 d	Frond doublings	Reduced	*L. punctata*	[101]
AgNP	93.52 nm (TEM); citrate coating; ζ –7.87 mV	OECD 221 medium; pH 5.5	5–160 µg/L	14 d	Frond number	Decreased (≥20 µg/L)	*Lemna minor*	[112]
					Growth rate	Decreased (≥10 µg/L)		
					Dry weight	Decreased (≥10 µg/L)		
					Growth inhibition	Increased		
AgNP	29.2 nm (TEM); citrate coating; ζ –7.87 mV	OECD 221 medium; pH 5.5	5–160 µg/L	14 d	Frond number	Decreased (≥80 µg/L)	*L. minor*	[112]
					Growth rate	Decreased (≥20 µg/L)		
					Dry weight	Decreased (≥20 µg/L)		
					Growth inhibition	Increased		
AgNP	7.8 nm; gum arabic coating; SSA 100 m^2/g; –49 mV to –	10% Hoagland's medium	0.5–10 mg/L	72 h	Fresh weight	Decreased (≥5 µg/L)	*Spirodela polyrhiza*	[54]

	44 mV				Dry weight	Decreased (≥5 µg/L)		
AgNP	240 nm; spherical; SSA 5–10 m^2/g; ζ –31.49 mV	Inorganic growth culture medium; pH 6.5; IS 4.25 mM	0.01–10 mg/L	7 d	Frond number Growth	Reduced Reduced	*L. gibba*	[106]
AgNP	5–20 nm (TEM); 84.97 nm (DLS); spherical; ζ –34.9 mV	Greenhouse water	8–128 µg/L	7 d	Frond number Growth rate Total weight Total fronds Growth inhibition	Decreased Decreased Decreased Decreased Increased	*L. minor*	[113]
AgNP	50 nm	Algal assay procedure medium; pH 7.5	0.1–200 mg/L	7 d	Growth rate	Decreased (≥1 mg/L)	*Lemna pausicostata*	[114]
TiO_2NP	2–3 nm	Algal assay procedure medium; pH 7.5; irradiance 6500–10 000 lx	31.25–500 mg/L	7 d	Growth rate	Decreased (≥250 mg/L)	*L. pausicostata*	[114]

TiO_2NP	275–2398 nm; SSA 50 m^2/g; ζ –25 mV to –20 mV (est.)	Steinburg growth medium; pH 5.5; $CaCO_3$ 166 mg/L; irradiance 5000 lx	0.01–10 mg/L	7 d	Frond number Growth rate	No effects No effects	*L. minor*	[74]
ZnONP	25 nm; SSA 90 m^2/g	Hoagland's medium; pH 6.5	1–50 mg/L	7 d	Growth rate Frond number Relative frond number	All inhibited at 50 mg/L	*Salvinia natans*	[55]
ZnONP	25 nm; SSA 90 m^2/g	OECD medium; pH 6.5	1–50 mg/L	7 d	Growth rate	No effects	*S. natans*	[58]
Al_2O_3NP	9.01 nm (TEM); 165–189 nm (NTA); SSA 200 m^2/g; spherical to void; ζ 5.3 mV	50% Hutner's medium; pH 5.3	10–1000 mg/L	7 d	Biomass	Stimulated	*L. minor*	[111]

ENP = engineered nanoparticle; CuONP = copper oxide nanoparticle; CdS QDs = cadmium sulfide quantum dots; AgNP = silver nanoparticle; TiO_2NP = titanium oxide nanoparticle; ZnOP = zinc oxide nanoparticle; Al_2O_3NP = aluminium oxide nanoparticle; SSA = specific surface area; TEM = transmission electron microscopy; SMPS = scanning mobility particle sizer; BET = Brunauer–Emmett–Teller method; IS = ionic strength; OECD = Organisation for Economic Co-operation and Development; DLS = dynamic light scattering; SSA = specific surface area; NTA = nanoparticle tracking analysis; ζ = zeta potential.

approximately 14 times more soluble than the former. A comparative study [101] between $CuCl_2$ (0.2 mg/L, 0.6 mg/L) and CuONPs (1 mg/L) on frond doublings and numbers indicated that CuONPs had similar toxicity to 0.6 mg/L $CuCl_2$. The toxicity of $CuCl_2$ was observed to be exposure concentration-dependent. The authors suggested that CuONPs were less soluble than $CuCl_2$ and that agglomerates were probably too large for internalization and, thus, adsorbed onto plant surfaces, while dissolved Cu was likely released from adsorbed CuONPs fractions. Zhang et al. [75] exposed *S. tabernaemontani* to CuONPs (0.5–50 mg/L) and Cu^{2+} (0.06 mg/L) for 21 d. Plants exposed to 0.5 mg/L and 50 mg/L CuONPs had 9% and 18% biomass reduction, respectively, after 21 d. However, exposure to either CuONPs or Cu^{2+} did not significantly reduce biomass compared with the control population, but CuONPs appeared more growth-inhibiting than Cu^{2+}.

AgNPs. Gubbins et al. [112] investigated the growth effects of 2 sizes of AgNPs (29 nm, 93 nm) and $AgNO_3$ using exposure concentrations of 5 µg/L to 160 µg/L for up to 14 d. Frond number, biomass (dry weight), and relative growth were assayed in the investigation. The toxicities of both AgNP forms and $AgNO_3$ on *L. minor* were dependent on exposure concentration and duration. The toxicity of soluble silver ($AgNO_3$) was higher compared with the 29-nm and 93-nm AgNP counterparts. The relatively higher toxicity of $AgNO_3$ was linked to predominating soluble Ag compared with AgNP exposures, where solubility was found to be <1% of exposure dosage. Hence, it was suggested that the uptake rate of dissolved Ag forms was higher than that of AgNPs, which accounted for the higher toxicity potential. Notably, no size-induced toxicity differences were reported between AgNPs batches averaging 29 nm and 93 nm [112].

Similarly, $AgNO_3$ was more growth-inhibiting than AgNPs to *S. polyrhiza* following 72-

h exposure at 0.5 mg/L to 10 mg/L concentrations [54]. The observation was attributed to higher uptake and accumulation of dissolved Ag from $AgNO_3$ exposure, whereas the dissolution of AgNPs was <3% of the initial dose. Another investigation [113] similarly reported growth effects of AgNPs on *L. minor* as exposure concentration–dependent and duration-dependent in 8 µg/L to 128 µg/L for 7 d. Frond numbers and growth rate were assayed in their study. However, no elaboration on underlying mechanisms for the toxicity observed was provided. Kim et al. [114] also reported exposure concentration-dependent growth inhibition of *Lemna paucicostata* exposed to 0.1 mg/L to 200 mg/L AgNPs for 7 d. At test end, AgNP concentrations in the range of 1 mg/L to 50 mg/L significantly reduced *L. paucicostata* growth rate, with complete inhibition at ≥100 mg/L. In their study [114], there were no attempts to define the mechanistic drivers of the observed AgNP effects. However, a loss of total Ag in suspension after prolonged exposure was reported and hypothetically linked to AgNP agglomeration. In the investigation by Oukarroum et al. [106], where *L. gibba* was exposed to AgNPs (0.01–10 mg/L) for 7 d, frond number and growth were inhibited in a concentration-dependent manner. The results indicated that AgNPs reduced both growth and number of fronds as a result of cellular solubilization of internalized AgNPs, which in turn increased free radical activity and decreased free cellular viability. Dissolution of AgNPs appeared insignificant. After 24 h at 10 mg/L, soluble Ag was recorded at a mere 0.15 mg/L, although more soluble Ag could be released as the study progressed. Therefore, AgNP toxicity was probably mostly nano driven.

TiO_2NPs. *Lemna minor* exposed to 0.1 mg/L to 5 mg/L TiO_2NPs for 7 d did not exhibit growth effects when assayed for growth rate and frond number [74]. Agglomeration and loss of TiO_2NPs in suspension were argued as the basis for reduced bioavailability and probably toxicity reduction. The authors [74] suggested that the lack of toxicity effects (photosynthetic and

growth-related) was a result of poor TiO_2NP uptake as evidenced by electron microscopy–based results, indicating no internalized TiO_2NP. Because TiO_2NPs are poorly soluble, their effects are probably caused by nano particulate activity. The results of Kim et al. [114] showed that TiO_2NPs at 250 mg/L and 500 mg/L significantly inhibited the *L. paucicostata* growth rate after 7 d. The induction of toxicity effects with increasing exposure dosage was suggested to be a result of an increasing accumulation rate of TiO_2NPs. Although ENPs tend to agglomerate with increasing concentration, leading to precipitation and sedimentation, in some instances increasing exposure concentration can promote adsorption of ENPs onto plant surfaces.

Al_2O_3NPs. Juhel et al. [111] exposed *L. minor* to up to 10 mg/L Al_2O_3NPs for 7 d and observed growth stimulation. The effect was linked to a nano effect after assessment of bulk aluminium, which was found not to be growth-inhibiting. The growth stimulation was not associated with Al^{3+} ions released because of Al_2O_3NP dissolution but partly as a result of enhancement of photosynthetic efficiency and root length, probably a counter-stress mechanism. The details on the mechanistic growth stimulation by nano alumina remain unclear and require further investigation.

ZnONPs. Overall toxicity of $ZnSO_4$ (3.5 mg/L) on *S. polyrhiza* was found to be higher than that of ZnONPs (1–50 mg/L) because of its elevated inhibition of growth rate, frond number, and biomass [55]. The higher solubility of $ZnSO_4$ than ZnONPs, allowing more rapid uptake, was put forward as the reason for the former being more toxic. It was suggested that agglomeration led to a reduction of ZnONP bioavailability in suspension, consequently suppressing bioavailability and toxicity. Higher growth effects of $ZnSO_4$ relative to ZnONPs have also been reported by others [58]. No significant growth effects were observed in *S. natans* exposed to ZnONPs, whereas $ZnSO_4$ caused growth inhibition [58]. Both studies suggested that

$ZnSO_4$ was more soluble than ZnONPs; hence, the former was more bioavailable and toxic [55,58]. Note that the studies used different exposure media.

CdS QDs. Following 21-d exposure to CdS QDs (0.5–50 mg/L), *S. tabernaemontani* experienced biomass reduction, and the effect was found to be dosage-dependent [75]. The plants had 31% biomass reduction at an exposure concentration of 5 mg/L and 44% at 50 mg/L. The toxicity of CdS QDs was hypothesized to arise from interactions with CdS QDs and dissolved Cd, but it is unclear which was predominant.

Summary: Toxicity effects. The toxicity literature reviewed points to the toxicity of metal-based ENPs as a result of soluble metallic forms, nano forms, or even both. When compared at similar exposure concentrations, soluble metallic forms are rapidly accumulated and therefore more toxic than nano forms. Notably for both forms, the toxicity is directly related to exposure concentration. As a key discriminator between metal-based ENPs and other types of ENMs, solubility seems to be an important regulator of their toxicity. Therefore, relatively soluble ENPs (e.g., ZnONPs) tend to be more toxic than poorly soluble forms (e.g., TiO_2NPs). However, one should treat such generalizations with caution. When it comes to oxidative stress endpoints, for example, the toxicity of nano forms tends to be higher than that of their soluble counterparts, especially for poorly soluble ENPs such as AgNPs and TiO_2NPs. It is also important to factor in persistent and slow release of soluble forms by ENPs when assessing the hazard of nano versus soluble metal forms. Furthermore, size, surface chemistry, and other characteristics of ENPs may influence their toxicity potential.

No reports investigated the additional influences of exposure and environmental water physicochemical conditions. The effect of photoactivity of TiO_2NPs on aquatic higher plants is another gap in the literature, requiring attention because of its effects on the photosynthetic

pathway.

SUMMARY AND FUTURE PERSPECTIVES

The present review suggests that the interactions of ENPs with aquatic higher plants are influenced by the interplay of numerous parameters under 3 broad categories: characteristics of ENPs, environmental water properties, and plant characteristics (physiological and anatomical). Diverse experimental protocols and instrumentation were adopted in the reviewed investigation (Tables 1–5), and commonalities among the protocols were rare. This raises challenges regarding data comparability, uniformity, and usability. Therefore, we recommend the development and adoption of standardized testing protocols to identify key focus parameters and improve data comparability to enhance the quality of data that support risk assessment of ENPs detrimental to aquatic higher plants. Despite these misgivings, we provide the following salient perspectives of the current information portfolio, with the hope that they will also contribute toward harmonization of test protocols.

Smaller ENPs tend to possess higher uptake potential by plants and in turn higher toxicity than their larger counterparts do, as demonstrated in numerous studies reviewed. The main controlling factors are the complex dynamics of bioavailability linked to ENP size and exposure media chemistry. The bioavailable size at the site of interaction matters more than the ENP primary size. Small ENP bioavailable size alone does not imply effective uptake because plant physiological and phenotypic characteristics may also influence uptake. Collectively, the findings suggest a higher risk potential toward aquatic plants from smaller ENPs as a result of enhanced bioaccumulation and toxic effects. Besides the size of ENPs, their morphological and surface properties (e.g., coating) can significantly influence their interactions with aquatic higher

plants. However, details of these aspects are still required for an understanding of the physicochemical basis for the effects of surface coating and morphology. For instance, electron microscopy images can better illustrate the dynamics of interaction at the plant surface and tissue or cellular internalization as a factor of ENP morphology. Therefore, investigations on the role of ENP morphology in the uptake by plants are encouraged.

Current data suggest that exposure concentration influences ENP bioaccumulation and toxicity effects, generally in a direct proportional relationship. However, reporting of actual exposure concentrations as total or dissolved metal per volume or particle number per volume was often poor. This aspect is important for hazard evaluation and determination because dissolution and agglomeration of ENPs can alter exposure concentration. Therefore, future studies should carefully evaluate ENP dissolution to improve data quality and, in turn, the nature and extent of conclusions drawn. For example, dissolution of metal-based ENPs regulates their interaction with aquatic plants as internalization and accumulation rates from exposure to soluble metallic forms are often higher than from exposure to colloidal nano forms. Even when higher accumulation resulted from ENP exposure, this was ascribed to the higher dissolution rate of nano forms. Hence, nanotoxicity was often accounted for based on dissolved metal content, with little evidence provided for "nano" induced toxicity. Perhaps the bias toward interpreting toxicity effects as a consequence of dissolution could be ascribed to the current limited analytical ability to detect, characterize, and quantify ENPs in complex environmental matrices. A further benefit would be the systematic classification of ENPs into categories under which observed effects are the result of either solutes, particulates, or both. This will become a reality as the analytical ability to detect, characterize, and quantify ENPs in complex environmental matrices improves.

Overall, based on the literature reviewed, we conclude that the uptake dynamics of ENPs

are poorly understood. To date, very few studies have investigated the uptake of ENPs by plants, which is an important factor providing evidence of adsorption or internalization (Table 1). Rather, many studies used the bioaccumulated metal proportion, which is an indirect indicator that cannot distinguish between adsorbed and internalized ENP fractions. Bioaccumulation reports showed that aquatic higher plants can serve as reservoirs of ENPs and released soluble metals and potentially transfer such contaminants between trophic levels in aquatic ecosystems. This is independent of the accumulation pathway (adsorption/uptake). However, the bioaccumulation potential can be manipulated for phytoextraction of nano pollutants in water resources.

The current data provide a good basis for evaluating the potential risks of ENPs to aquatic higher plants. However, justification exists for additional research aimed at addressing the gaps identified to undertake risk evaluation under more realistic environmental exposure scenarios.

The wide range of testing protocols and species makes it difficult to draw meaningful conclusions about toxicity effects such as species sensitivity or endpoint sensitivity. In general, however, highly soluble ENPs appear likely to possess elevated toxicity effects, based on rapid uptake of dissolved metal forms. But nano driven toxicity cannot simply be overlooked, as shown by the high oxidative toxicity of AgNPs compared with soluble Ag. For ENPs known to be photoactive, the influence of exposure light intensity needs to be further studied and considered when interpreting findings. Furthermore, to harmonize future studies, a focus on photosynthetic and growth effects would be useful because studies in these areas tend to be more cost-effective than investigations of subcellular effects, which often require costly reagents. Subcellular studies could then be a component of higher-tier testing, following the assessment of

growth and photosynthetic effects.

Acknowledgment

M.Thwala acknowledges the UNESCO Keizo Obuchi Fellowship 2014 undertaken at Environmental Toxicology Unit, Clemson University (SC, USA) and the Thuthuka Programme of the National Research Foundation (South Africa). Sponsorship of the present work by the CSIR under the project "Nanotechnology Risk Assessment in Aquatic Systems: Experimental and Modelling Approaches" is also acknowledged. We also thank the editorial contribution provided by M. Silberbauer. The authors declare no conflict of interest.

Data availability—All the information used in the present review is cited. Furthermore, Tables 1–5 list studies which are cited in different sections of the article; therefore, such information is publicly available. No additional information is withheld by the authors.

REFERENCES

1. Colvin VL. 2003. The potential environmental impact of nanomaterials. *Nat Biotechnol* 21:1166–1170.

2. Oberdörster E. 2004. Manufactured nanomaterials (fullerenes, C_{60}) induce oxidative stress in the brain of juvenile largemouth bass. *Environ Health Perspect* 112:1058–1062.

3. Oberdörster G, Oberdörster E, Oberdörster J. 2005. Nanotoxicology: An emerging discipline evolving from studies of ultrafine particles. *Environ Health Perspect* 113:823–839.

4. Nel A, Xia T, Madler L, Li N. 2006. Toxic potential of materials at the nanolevel. *Science* 311:622–627.

5. Jolivet J, Froidefond C, Pottier A, Chanéac C, Cassaignon S, Tronc E, Euzen P. 2004. Size

tailoring of oxide nanoparticles by precipitation in aqueous medium. A semi-quantitative modelling. *J Mater Chem* 14:3281–3288.

6. Auffan M, Rose J, Proux O, Borschneck D, Masion A, Chaurand P, Hazemann JL, Chaneac C, Jolivet JP, Wiesner MR, Geen AV, Bottero JY. 2008. Enhanced adsorption of arsenic onto maghemites nanoparticles: As(III) as a probe of the surface structure and heterogeneity. *Langmuir* 24:3215–3222.

7. BCC Research. 2012. Nanotechnology: A realistic market assessment. NANO31E. Wellesley, MA, USA.

8. Consumer Products Inventory. 2015. Project on Emerging Nanotechnologies. [cited 2015 February 2]. Available from: http://www.nanotechproject.org/cpi/about/analysis/.

9. Benn TM, Westerhoff P. 2008. Nanoparticle silver released into water from commercially available sock fabrics. *Environ Sci Technol* 42:4133–4139.

10. Kaegi R, Voegelin A, Ort C, Sinnet B, Thalman B, Krismer J, Hagendorfer H, Elumelu M, Mueller E. 2013. Fate and transformation of silver nanoparticles in urban wastewater systems. *Water Res* 47:3866–3877.

11. Kirkegaard P, Hansen SF, Rygaard M. 2015. Potential exposure and treatment efficiency of nanoparticles in water supplies based on wastewater reclamation. *Environ Sci Nano* 2:191–202.

12. Musee N, Zvimba JN, Schaefer LM, Nota N, Sikhwivhilu LM, Thwala M. 2014. Fate and behavior of ZnO- and Ag-engineered nanoparticles and a bacterial viability assessment in a simulated wastewater treatment plant. *J Environ Sci Health A* 49:59–66.

13. Hund-Rinke K, Herrchen M, Schlich K. 2014. Integrative test strategy for the environmental assessment of nanomaterials. Project No. (FKZ) 3712 65 409. Federal Environment

Agency, Schmallenberg, Germany.

14. Kahru A, Ivask A. 2013. Mapping the dawn of nanoecotoxicological research. *Acc Chem Res* 46:823–833.

15. Donaldson K, Stone V, Tran CL, Kreyling W, Borm PJA. 2004. Nanotoxicology. *Occup Environ Med* 61:727–728.

16. Kreyling W, Semmler-Behnke M, Möller W. 2006. Health implications of nanoparticles. *J Nanopart Res* 8:543–562.

17. Baun A, Hartmann NB, Grieger K, Kusk KO. 2008. Ecotoxicity of nanoparticles to aquatic invertebrates: A brief review and recommendations for future toxicity testing. *Ecotoxicology* 17:387–395.

18. Xia T, Li N, Nel AE. 2009. Potential health impact of nanoparticles. *Annu Rev Public Health* 30:137–150.

19. Oberdörster E, Zhu SQ, Blickley TM, Clellan-Green P, Haasch ML. 2006. Ecotoxicology of carbon-based engineered nanoparticles: Effects of fullerene (C_{60}) on aquatic organisms. *Carbon* 44:1112–1120.

20. Handy RD, Shaw BJ. 2007. Toxic effects of nanoparticles and nanomaterials: Implications for public health, risk assessment and the public perception of nanotechnology. *Health Risk Soc* 9:125–144.

21. Moore MN. 2006. Do nanoparticles present ecotoxicological risks for the health of the aquatic environment? *Environ Int* 32:967–976.

22. Kahru A, Dubourguier HC. 2010. From ecotoxicology to nano-ecotoxicology. *Toxicology* 269:105–119.

23. Behra R, Krug H. 2008. Nanoecotoxicology: Nanoparticles at large. *Nat Nanotechnol* 3:253–

254.

24. Handy RD, von der Kammer F, Lead JR, Martin Hassellov M, Richard Owen R, Crane M. 2008. The ecotoxicology and chemistry of manufactured nanoparticles. *Ecotoxicology* 17:287–314.

25. Klaine SJ, Alvarez PJJ, Batley GE, Fernandes TF, Handy RD, Lyon DY, Mahendra S, Mclaughlin MJ, Lead JR. 2008. Nanomaterials in the environment: Behaviour, fate, bioavailability, and effects. *Environ Toxicol Chem* 27:1825–1851.

26. Heinlaan M, Ivask A, Blinova I, Dubourguier H, Kahru A. 2008. Toxicity of nanosized and bulk ZnO, CuO and TiO_2 to bacteria *Vibrio fischeri* and crustaceans *Daphnia magna* and *Thamnocephalus platyurus. Chemosphere* 71:1308–1316.

27. Barnes RJ, van der Gast C, Riba O, Lehtovirta LE, Prosse JI, Dobson PJ, Thompson IP. 2010. The impact of zero-valent iron nanoparticles on a river water bacterial community. *J Hazard Mater* 184:73–80.

28. Musee N, Thwala M, Nota N. 2011. The antibacterial effects of engineered nanomaterials: Implications for wastewater treatment plants. *J Environ Monit* 13:1164–1183.

29. von Moos N, Bowen P, Slaveykova VI. 2014. Bioavailability of inorganic nanoparticles to planktonic bacteria and aquatic microalgae in freshwater. *Environ Sci Nano* 1:214–232.

30. Ji J, Long Z, Lin D. 2011. Toxicity of oxide nanoparticles to the green algae *Chlorella* sp. *Chem Eng J* 170:525–530.

31. Quigg A, Chin W, Chen C, Zhang S, Joang Y, Miao A, Schwer KA, Xu C, Santchi PH. 2013. Direct and indirect toxic effects of engineered nanoparticles on algae: Role of natural organic matter. *ACS Sustain Chem Eng* 1:686–702.

32. Lovern SB, Owen HA, Klaper R. 2008. Electron microscopy of gold nanoparticle intake in

the gut of *Daphnia magna*. *Nanotoxicology* 2:43–48.

33. Li T, Albee B, Alemayehu M, Diaz R, Ingahm L, Kamal S, Rodriguez M, Bishnoi SW. 2010. Comparative toxicity study of Ag, Au, and Ag–Au bimetallic nanoparticles on *Daphnia magna*. *Anal Bioanal Chem* 398:689–700.

34. Lee B, Ranville JF. 2012. The effect of hardness on the stability of citrate-stabilized gold nanoparticles and their uptake by *Daphnia magna*. *J Hazard Mater* 213–214:434–439.

35. Wray AT, Klaine SJ. 2015. Modeling the influence of physicochemical properties of gold nanoparticle uptake and elimination by *Daphina magna*. *Environ Sci Technol* 34:860–872.

36. Johnston BD, Scown TS, Moder J, Cumberland SA, Baalousha M, Linge K, van Aerle R, Jarvis K, Lead JR, Tyler CR. 2010. Bioavailability of nanoscale metal oxides TiO_2, CeO_2, and ZnO to fish. *Environ Sci Technol* 44:1144–1151.

37. Shaw BJ, Handy RD. 2011. Physiological effects of nanoparticles on fish: A comparison of nanometals versus metal ions. *Environ Int* 37:1083–1097.

38. He X, Aker WG, Hwang H. 2014. An in vivo study on the photo-enhanced toxicities of S-doped TiO_2 nanoparticles to zebrafish embryos (*Danio rerio*) in terms of malformation, mortality, rheotaxis dysfuntion, and DNA damage. *Nanotoxicology* 8:185–195.

39. Lahive E, O'Halloran J, Jansen M. 2014. A marriage of convenience; a simple food chain comprised of *Lemna minor* (L.) and *Gammarus pulex* (L.) to study the dietary transfer of zinc. *Plant Biol* 17:75–81.

40. Peralta-Videa JR, Zhao L, Lopez-Moreno ML, de la Rosa G, Hong J, Gardea-Torresdey JL. 2011. Nanomaterials and the environment: A review for the biennium 2008–2010. *J Hazard Mater* 186:1–15.

41. Miralles P, Church TL, Harris AT. 2012. Toxicity, uptake, and translocation of engineered

nanomaterials in vascular plants. *Environ Sci Technol* 46:9224–9239.

42. Glenn JB, Klaine SJ. 2013. Abiotic and biotic factors that influence the bioavailability of gold nanoparticles to aquatic macrophytes. *Environ Sci Technol* 47:10223–10230.

43. Ma H, Williams PL, Diamond SA. 2013. Ecotoxicity of manufactured ZnO nanoparticles: A review. *Environ Pollut* 172:76–85.

44. Thwala M, Musee N, Sikhwivhilu LM, Wepener V. 2013. The oxidative toxicity of Ag and ZnO nanoparticles towards the aquatic plant *Spirodela punctuta* and the role of testing media parameters. *Environ Sci Process Impacts* 15:1830–1843.

45. Glenn JB, White SA, Klaine SJ. 2012. Interactions of gold nanoparticles with aquatic macrophytes are size and species dependent. *Environ Toxicol Chem* 31:194–201.

46. Holden PA, Nisbet RM, Lenihan HS, Miller RJ, Cherr GN, Schimel JP, Gardea-Torresdey JL. 2013. Ecological nanotoxicology: Integrating nanomaterial hazard considerations across the subcellular, population, community, and ecosystems levels. *Acc Chem Res* 46:813–822.

47. Fairbrother A, Wenstell R, Sappington K, Wood W. 2007. Framework for metals analysis. *Ecotoxicol Environ Saf* 68:145–227.

48. Delay M, Frimmel FH. 2012. Nanoparticles in aquatic systems. *Anal Bioanal Chem* 402:583–592.

49. Unrine JM, Colman BP, Bone AJ, Gondikas AP, Matson CW. 2012. Biotic and abiotic interactions in aquatic microcosms determine fate and toxicity of Ag nanoparticles. Part 1. Aggregation and dissolution. *Environ Sci Technol* 46:6915–6924.

50. Stone V, Nowack B, Baun A, van den Brink N, von der Kammer F, Dusinska M, Handy R, Hankin S, Hassellöv M, Joner E, Fernandes TF. 2010. Nanomaterials for environmental

studies: Classification, reference material issues, and strategies for physico-chemical characterisation. *Sci Tot Environ* 408:1745–1754.

51. Nowack B, Ranville JF, Diamond S, Gallego-Urrea JA, Metcalfe C, Rose J, Horne N, Koelmans AA, Klaine SJ. 2012. Potential scenarios for nanomaterials release and subsequent alteration in the environment. *Environ Toxicol Chem* 31:50–59.

52. Auffan M, Rose J, Wiesner MR, Bottero J. 2009. Chemical stability of metallic nanoparticles: A parameter controlling their potential cellular toxicity in vitro. *Environ Pollut* 157:1127–1133.

53. Bone AJ, Colman BP, Gondikas AP, Newton KM, Harrold KH, Cory RM, Unrine JM, Klaine SJ, Matson CW, Di Giulio RT. 2012. Biotic and abiotic interactions in aquatic microcosms determine fate and toxicity of Ag nanoparticles: Part 2. Toxicity and Ag speciation. *Environ Sci Technol* 46:6925–6933.

54. Jiang H, Li M, Chang F, LI W, Yin L. 2012. Physiological analysis of silver nanoparticles and $AgNO_3$ toxicity to *Spirodela polyrhiza*. *Environ Toxicol Chem* 31:1880–1886.

55. Hu C, Liu Y, Li X, Li M. 2013. Biochemical responses of duckweed (*Spirodela polyrhiza*) to zinc oxide nanoparticles. *Arch Environ Contam Toxicol* 64:643–651.

56. Yeo M, Nam D. 2013. Influence of different types of nanomaterials on their bioaccumulation in a paddy microcosm: A comparison of TiO_2 nanoparticles and nanotubes. *Environ Pollut* 178:166–172.

57. Yin L, Cheng Y, Espinasse B, Colman BP, Auffan M, Wiesner M, Rose J, Liu J, Bernhardt ES. 2011. More than the ions: The effects of silver nanoparticles on *Lolium multiflorum*. *Environ Sci Technol* 45:2360–2367.

58. Hu C, Liu X, Li X, Zhao Y. 2014. Evaluation of growth and biochemical indicators of

Salvinia natans exposed to zinc oxide nanoparticles and zinc accumulation in plants. *Environ Sci Pollut Res* 21:732–739.

59. Stebounova LS, Guio E, Grassian VH. 2011. Silver nanoparticles in simulated biological media: A study of aggregation, sedimentation, and dissolution. *J Nanopart Res* 13:233–244.

60. Remedios C, Rosario F, Bastos V. 2012. Environmental nanoparticles interactions with plants: Morphological, physiological, and genotoxic aspects. *J Bot* 2012:1–8.

61. Delay M, Dolt T, Woellhaf A, Sembritzki R, Frimmel FH. 2011. Interactions and stability of silver nanoparticles in the aqueous phase: Influence of natural organic matter (NOM) and ionic strength. *J Chromatogr A* 1218:4206–4212.

62. Fabrega J, Luoma SM, Tyler CR, Galloway TS, Lead JR. 2011. Silver nanoparticles: Behaviour and effects in the aquatic environment. *Environ Int* 37:517–531.

63. Levard C, Hotze EM, Lowry GV, Brown GE Jr. 2012. Environmental transformations of silver nanoparticles: Impact on stability and toxicity. *Environ Sci Technol* 46:6900–6914.

64. Fatehah MO, Aziz HA, Stoll S. 2014. Nanoparticle properties, behaviour, fate in aquatic systems and characterisation methods. *J Coll Sci Biotechnol* 3:1–30.

65. Bian S, Mudumkotuwa IA, Rupasinghe T, Grassian VH. 2011. Aggregation and dissolution of 4 nm ZnO nanoparticles in aqueous environments: Influence of pH, ionic strength, size, and adsorption of humic acid. *Langmuir* 27:6059–6068.

66. Campbell PGC. 1995. Interactions between trace metals and aquatic organisms: A critique of the free-ion activity model. In Tessier A, Turner DR, eds, *Metal Speciation and Bioavailability in Aquatic Systems*. Wiley, Chichester, UK, pp 45–102.

67. Reed RB, Ladner DA, Higgins CP, Westerhoff P, Ranville JF. 2012. Solubility of nano-zinc

oxide in environmentally and biologically important matrices. *Environ Toxicol Chem* 31:93–99.

68. Turner T, Brice D, Brown MT. 2012. Interactions of silver nanoparticles with the marine macroalga *Ulva lactuta*. *Ecotoxicology* 21:148–154.

69. Chernousova S, Epple M. 2013. Silver as antibacterial agent: Ion, nanoparticle, and metal. *Angew Chem Int Edit* 52:1636–653.

70. Luyts K, Napierska D, Nemery B, Hoet PHM. 2013. How physico-chemical characteristics of nanoparticles cause their toxicity: Complex and unresolved interrelations. *Environ Sci Process Impacts* 15:23–38.

71. Odzak N, Kistler D, Behra R, Sigg L. 2014. Dissolution of metal and metal oxide nanoparticles in aqueous media. *Environ Pollut* 191:132–138.

72. Ma X, Geiser-Lee J, Deng Y, Kolmakov A. 2010. Interactions between engineered nanoparticles (ENPs) and plants: Phytotoxicity, uptake and accumulation. *Sci Total Environ* 408:3053–3061.

73. Nair R, Varghese SH, Nair BG, Maekawa T, Yoshida Y, Kumar DS. 2010. Nanoparticulate material delivery to plants. *Plant Sci* 179:154–163.

74. Li L, Sillanpaa M, Tuominen M, Lounatmaa K, Schultz E. 2013. Behavior of titanium dioxide nanoparticles in *Lemna minor* growth test conditions. *Ecotoxicol Environ Saf* 88:89–94.

75. Zhang D, Hua T, Xiao F, Chen C, Gersberg RM, Liu Y, Ng WJ, Tan SK. 2014. Uptake and accumulation of CuO nanoparticles and CdS/ZnS quantum dot nanoparticles by *Schoenoplectus tabernaemontani* in hydroponic mesocosms. *Ecol Eng* 70:114–123.

76. Dietz K, Herth S. 2011. Plant nanotoxicology. *Trends Plant Sci* 16:582–589.

77. Sabo-Attwood T, Unrine JM, Stone JW, Murphy CJ, Ghoshroy S, Blom D, Bertsch PM, Newman LA. 2011. Uptake, distribution and toxicity of gold nanoparticles in tobacco (*Nicotiana xanthi*) seedlings. *Nanotoxicology* 6:353–360.

78. Lin D, Xing B. 2008. Root uptake and phytotoxicity of ZnO nanoparticles. *Environ Sci Technol* 42:5580–5585.

79. Carpita N, Sabularse D, Montezinos D, Delmer DP. 1979. Determination of the pore size of cell walls of living plant cells. *Science* 205:1144–1147.

80. Adani F, Papa G, Schievano A, Cardinale G, D'Imporzano G, Tambone F. 2011. Nanoscale structure of the cell wall protecting cellulose from enzyme attack. *Environ Sci Technol* 45:1107–1113.

81. Judy JD, Unrine JM, Rao W, Wirick S, Bertsch PM. 2012. Bioavailability of gold nanomaterials to plants: importance of particle size and surface coating. *Environ Sci Technol* 46:8467–8474.

82. Rico CM, Majumdar S, Duarte-Gardea M, Peralta-Videa JR, Gardea-Torresdey JL. 2011. Interaction of nanoparticles with edible plants and their possible implications in the food chain. *J Agric Food Chem* 59:3485–3498.

83. Yruela I. 2009. Copper in plants: Acquisition, transport and interactions. *Funct Plant Biol* 36:409–430.

84. Festa RA, Thiele DJ. 2011. Copper: An essential metal in biology. *Curr Biol* 21:877–883.

85. Etxeberria E, Gonzalez P, Baroja-Fernandez E, Pozueta-Romero J. 2006. Fluid-phase uptake of artificial nano-spheres and fluorescent quantum-dots by sycamore cultured cells. *Plant Signal Behav* 1:181–185.

86. Liu Q, Chen B, Wang Q, Shi X, Xiao Z, Lin J, Fang X. 2009. Carbon nanotubes as molecular

transporters for walled plant cells. *Nano Lett* 9:1007–1010.

87. Smirnova E, Gusev A, Zaytseva O. 2012. Uptake and accumulation of multiwalled carbon nanotubes change the morphometric and biochemical characteristics of *Onobrychis arenaria* seedlings. *Front Chem Sci Eng* 6:132–138.

88. Bian J, Berninger JP, Fulton BA, Brooks BE. 2013. Nutrient stoichiometry and concentrations influence silver toxicity in the aquatic macrophyte *Lemna gibba*. *Sci Total Environ* 449:229–236.

89. Aslani F, Bagheri S, Julkapli NM, Juraimi AS, Hashemi FS, Baghdadi A. 2014. Effects of engineered nanomaterials on plant growth: An overview. *Sci World J* 449:1–28.

90. Kurepa J, Paunesku T, Vogt S, Arora H, Rabatic BM, Lu J, Wanzer MB, Woloschak GE, Smalle JA. 2010. Uptake and distribution of ultrasmall anatase TiO_2 alizarin red S nanoconjugates in *Arabidopsis thaliana*. *Nano Lett* 10:2296–2302.

91. Lee CW, Mahendra S, Zodrow K, Li D, Tsai YC, Braam J, Alvarez PJJ. 2010. Developmental phytotoxicity of metal oxide nanoparticles to *Arabidopsis thaliana*. *Environ Toxicol Chem* 29:669–675.

92. Lin S, Reppert J, Hu Q, Hunson JS, Reid ML, Ratnikova T. 2009. Uptake, translocation and transmission of carbon nanomaterials in rice plants. *Small* 5:1128–1132.

93. Chen R, Ratnikova TA, Stone MB, Lin S, Lard M, Huang G, Hudson JS, Ke PC. 2010. Differential uptake of carbon nanoparticles by plant and mammalian cells. *Small* 6:612–617.

94. Perreault F, Samadani M, Dewez D. 2014. Effect of soluble copper released from copper oxide nanoparticles solubilisation on growth and photosynthetic processes of *Lemna gibba*. *Nanotoxicol* 8:374–382.

95. Dhir B, Sharmila P, Saradhi PP, Nasim SA. 2009. Physiological and antioxidant responses of *Salvinia natans* exposed to chromium-rich wastewater. *Ecotoxicol Environ Saf* 72:1790–1797.

96. Prado C, Rodríguez-Montelongo L, González JA, Pagano EA, Hilal M, Prado FE. 2010. Uptake of chromium by *Salvinia minima*: Effect on plant growth, leaf respiration and carbohydrate metabolism. *J Hazard Mater* 177:546–553.

97. Oliver JD. 1993. A review of the biology of giant *Salvinia*. *J Aquat Plant Manag* 31:227–231.

98. Smith AR, Pryer KM, Schuettpelz E, Korall P, Schneider H, Wolf PG. 2006. A classification for extant ferns. *Taxonomy* 55:705–731.

99. Perreault F, Popovic R, Dewez D. 2014. Different toxicity mechanisms between bare and polymer-coated copper oxide nanoparticles in *Lemna gibba*. *Environ Pollut* 185:219–227.

100. Perreault F, Oukarroum A, Melegari SP, Matias WG, Popovic R. 2012. Polymer coating of copper oxide nanoparticles increases nanoparticles uptake and toxicity in the green alga *Chlamydomonas reinhardtii*. *Chemosphere* 87:1388–1394.

101. Shi J, Abid AD, Kennedy IM, Hristova KR, Silk WK. 2011. To duckweeds (*Landoltia punctata*), nanoparticulate copper oxide is more inhibitory than the soluble copper in the bulk solution. *Environ Pollut* 159:1277–1282.

102. Ferry JL, Craig P, Hexel C, Sisco P, Frey R, Pennington PL, Fulton MH, Scott IG, Decho AW, Kashiwada S, Murphy CJ, Shaw T. 2009. Transfer of gold nanoparticles from the water column to the estuarine food web. *Nat Nanotechnol* 4:441–444.

103. Burns JM, Pennington PL, Sisco PN, Frey R, Kashiwada S, Fulton MH, Scott GI, Decho AW, Murphy CJ, Shaw TJ, Ferry JL. 2013. Surface charge controls the fate of Au nanorods

in saline estuaries. *Environ Sci Technol* 47:12844–12851.

104. Griffitt RJ, Luo J, Gao J, Bonzongo J, Barber DS. 2008. Effects of particle composition and species on toxicity of metallic nanomaterials in aquatic organisms. *Environ Toxicol Chem* 27:1972–1978.

105. Liu J, Wang Z, Liu FD, Kane AB, Hurt BH. 2012. Chemical transformations of nanosilver in biological environments. *ACS Nano* 6:9887–9899.

106. Oukarroum A, Barhoumi L, Pirastru L, Dewez D. 2013. Silver nanoparticle toxicity effects on growth and cellular viability of the aquatic plant *Lemna gibba*. *Environ Toxicol Chem* 32:902–907.

107. Jiang H, Qiu X, Li G, Li W, Yin L. 2014. Silver nanoparticles induced accumulation of reactive oxygen species and alteration of antioxidant systems in the aquatic plant *Spirodela polyrhiza*. *Environ Toxicol Chem* 33:1398–1405.

108. McGeer JM, Brix KV, Skeaff JM, DeForest DK, Brigham SI, Adams WJ, Green A. 2003. Inverse relationship between bioconcentration factor and exposure concentration for metals: Implications for hazard assessment of metals in the aquatic environment. *Environ Toxicol Chem* 22:1017–1037.

109. Song G, Gao Y, Wu H, Hou W, Zhang C, Ma H. 2012 . Physiological effect of anatase TiO_2 nanoparticles on *Lemna minor*. *Environ Toxicol Chem* 31:2147–2152.

110. Maksymiec W. 1997. Effect of copper on cellular processes in higher plants. *Photosynthetica* 34:321–342.

111. Juhel G, Batisse E, Hugues Q, Daly D, van Pelt F, O'Halloran J, Jansen MAK. 2011. Alumina nanoparticles enhance growth of *Lemna minor*. *Aqua Toxicol* 105:328–336.

112. Gubbins EJ, Batty LC, Lead JR. 2011. Phytotoxicity of silver nanoparticles to *Lemna minor*

L. *Environ Pollut* 159:1551–1559.

113. Ucuncu E, Ozkan AD, Kursungoz C, Ulger ZE, Olmez TT, Tekinay T, Ortac B, Tunca E. 2014. Effects of laser ablated silver nanoparticles on *Lemna minor*. *Chemosphere* 108:251–257.

114. Kim E, Kim S, Kim H, Lee SG, Lee SJ, Jeong SW. 2011. Growth inhibition of aquatic plant caused by silver and titanium oxide nanoparticles. *Toxicol Environ Health Sci* 3:1–6.

.